

AD-A243 077



Hydro Research Center

Bethesda, Maryland 20084-5000

DTRC/SHD-1361-01 August 1991

Ship Hydromechanics Department

Departmental Report

DTRC/SHD-1361-01 A Frequency-Domain Method for Estimating the Incidence and Severity of Sliding

A Frequency-Domain Method for Estimating the Incidence and Severity of Sliding

by Ross Graham, A. Erich Baitis, William G. Meyers

DTIC ELECTE DEC 09 1991 S B D



Approved for public release: Distribution unlimited.

91-17285



91 17 285

## MAJOR DTRC TECHNICAL COMPONENTS

- CODE 011 DIRECTOR OF TECHNOLOGY, PLANS AND ASSESSMENT
  - 12 SHIP SYSTEMS INTEGRATION DEPARTMENT
  - 14 SHIP ELECTROMAGNETIC SIGNATURES DEPARTMENT
  - 15 SHIP HYDROMECHANICS DEPARTMENT
  - 16 AVIATION DEPARTMENT
  - 17 SHIP STRUCTURES AND PROTECTION DEPARTMENT
  - 18 COMPUTATION, MATHEMATICS & LOGISTICS DEPARTMENT
  - 19 SHIP ACOUSTICS DEPARTMENT
  - 27 PROPULSION AND AUXILIARY SYSTEMS DEPARTMENT
  - 28 SHIP MATERIALS ENGINEERING DEPARTMENT

### DTRC ISSUES THREE TYPES OF REPORTS:

1. **DTRC reports, a formal series**, contain information of permanent technical value. They carry a consecutive numerical identification regardless of their classification or the originating department.
2. **Departmental reports, a semiformal series**, contain information of a preliminary, temporary, or proprietary nature or of limited interest or significance. They carry a departmental alphanumeric identification.
3. **Technical memoranda, an informal series**, contain technical documentation of limited use and interest. They are primarily working papers intended for internal use. They carry an identifying number which indicates their type and the numerical code of the originating department. Any distribution outside DTRC must be approved by the head of the originating department on a case-by-case basis.

UNCLASSIFIED

SECURITY CLASSIFICATION OF THIS PAGE

REPORT DOCUMENTATION PAGE				Form Approved OMB No 0704-0188	
1a REPORT SECURITY CLASSIFICATION <b>UNCLASSIFIED</b>		1b RESTRICTIVE MARKINGS			
2a SECURITY CLASSIFICATION AUTHORITY		3 DISTRIBUTION / AVAILABILITY OF REPORT  Approved for public release: Distribution unlimited.			
2b DECLASSIFICATION / DOWNGRADING SCHEDULE					
4 PERFORMING ORGANIZATION REPORT NUMBER(S)  DTRC/SHD-1361-01		5 MONITORING ORGANIZATION REPORT NUMBER(S)			
6a. NAME OF PERFORMING ORGANIZATION David Taylor Research Center Ship Hydromechanics Dept.		6b OFFICE SYMBOL (if applicable) Code 1561	7a NAME OF MONITORING ORGANIZATION		
6c. ADDRESS (City, State, and ZIP Code)  Bethesda, Maryland 20084-5000		7b ADDRESS (City, State, and ZIP Code)			
8a. NAME OF FUNDING / SPONSORING ORGANIZATION Chief of Naval Research		8b OFFICE SYMBOL (if applicable) ONT 211	9 PROCUREMENT INSTRUMENT IDENTIFICATION NUMBER		
8c. ADDRESS (City, State, and ZIP Code)  Arlington, Virginia 22217-5000		10 SOURCE OF FUNDING NUMBERS			
		PROGRAM ELEMENT NO 62121N	PROJECT NO RH21S23	TASK NO 5	WORK UNIT ACCESSION NO DN178067
11. TITLE (Include Security Classification) <b>A FREQUENCY-DOMAIN METHOD FOR ESTIMATING THE INCIDENCE AND SEVERITY OF SLIDING</b>					
12. PERSONAL AUTHOR(S) <b>ROSS GRAHAM, A. ERICH BAITIS and WILLIAM G. MEYERS</b>					
13a. TYPE OF REPORT Final		13b TIME COVERED FROM <u>910101</u> TO <u>910830</u>	14 DATE OF REPORT (Year, Month, Day) 1991 August		15 PAGE COUNT 43
16 SUPPLEMENTARY NOTATION DTRC Work Unit No. 1-1506-122-10					
17 COSATI CODES			18 SUBJECT TERMS (Continue on reverse if necessary and identify by block number)		
FIELD	GROUP	SUB-GROUP	Seakeeping Criteria, Operability, Sliding		
19 ABSTRACT (Continue on reverse if necessary and identify by block number)					
<p>A frequency-domain method of predicting the incidence of personnel or equipment sliding is presented which includes the (linearized) forces due to roll, pitch, longitudinal, lateral and vertical accelerations, and also the effects of non-zero mean heel. The predictions of the method are compared with the results of observations of at-sea sliding incidents, and good correspondence is obtained.</p> <p>A simple approximation for the duration of threshold exceedance probability density is described, and used to develop a method for predicting the incidence of slides greater than a certain severity. The method applies for arbitrary lateral and vertical acceleration, but only to the case in which the longitudinal acceleration is negligible. An example of the application of the method is presented.</p> <p>It is argued that ship motions such as roll, pitch, lateral and longitudinal accelerations are the wrong physical parameters for expressing seakeeping criteria. These criteria become simpler when expressed in terms of the incidence of degrading events such as helicopters sliding, and are equally applicable to all vessel types.</p>					
20 DISTRIBUTION / AVAILABILITY OF ABSTRACT <input type="checkbox"/> UNCLASSIFIED/UNLIMITED <input checked="" type="checkbox"/> SAME AS RPT <input type="checkbox"/> DTIC USERS			21 ABSTRACT SECURITY CLASSIFICATION <b>UNCLASSIFIED</b>		
22a NAME OF RESPONSIBLE INDIVIDUAL A. Erich Baitis			22b TELEPHONE (Include Area Code) 301-227-1627	22c OFFICE SYMBOL Code 1561	

DD Form 1473, JUN 86

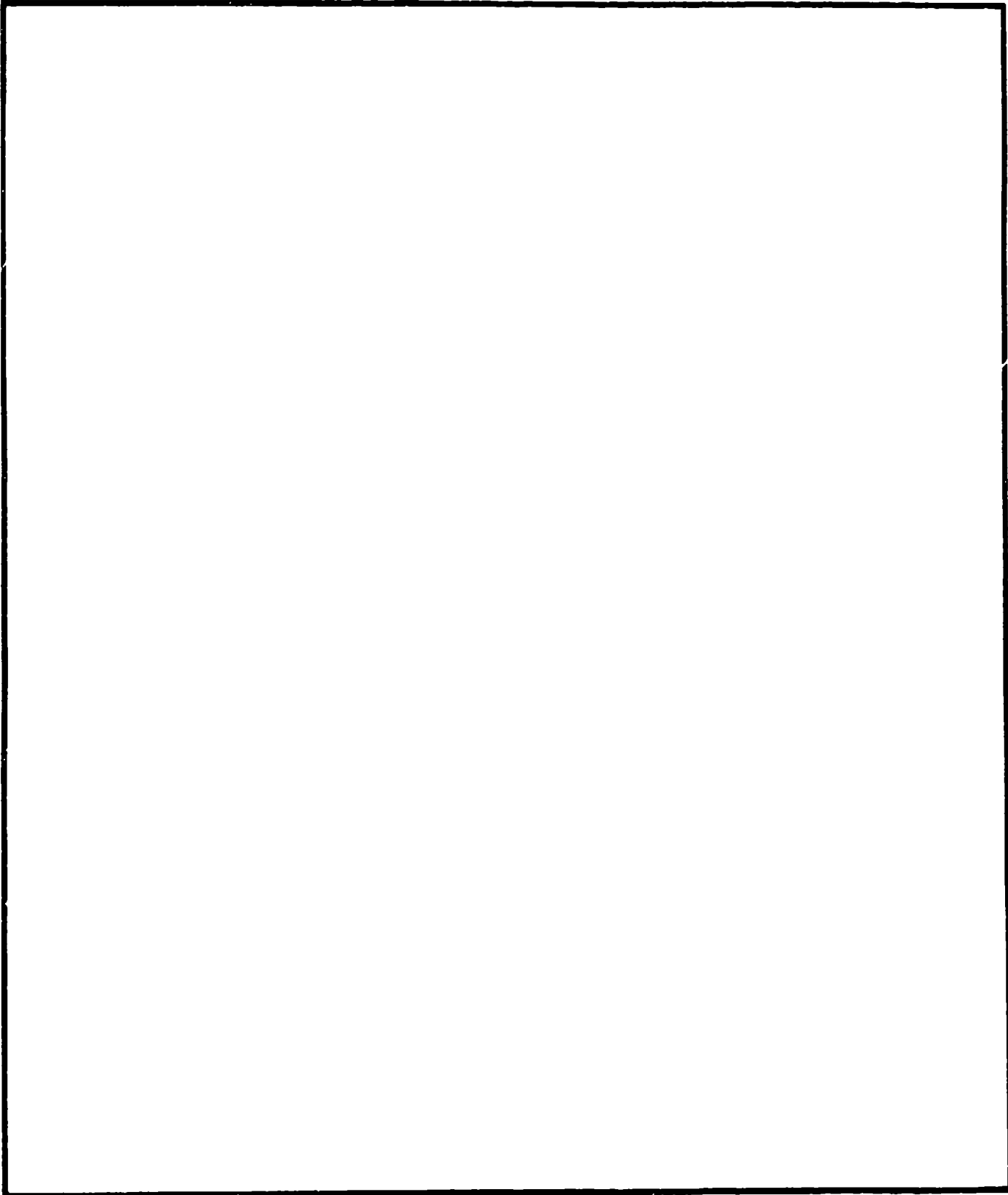
Previous editions are obsolete

S/N 0102-LF-014-6603

SECURITY CLASSIFICATION OF THIS PAGE

UNCLASSIFIED

SECURITY CLASSIFICATION OF THIS PAGE



## CONTENTS

	Page
NOMENCLATURE . . . . .	v
ABSTRACT . . . . .	1
ADMINISTRATIVE INFORMATION . . . . .	1
INTRODUCTION . . . . .	1
PREDICTION OF SLIDING INCIDENCE WITH ZERO LONGITUDINAL AC- CELERATION . . . . .	3
COMPARISON OF MEASURED AND PREDICTED SLIDING INCIDENCE .	5
PREDICTION OF SLIDING SEVERITY WITH ZERO LONGITUDINAL AC- CELERATION . . . . .	8
REGULAR WAVE CASE . . . . .	8
IRREGULAR WAVE CASE . . . . .	10
PREDICTION OF SLIDING INCIDENCE WITH NONZERO LONGITUDI- NAL ACCELERATION . . . . .	12
CONCLUDING REMARKS . . . . .	16
ACKNOWLEDGEMENTS . . . . .	17
APPENDIX A - A SIMPLE APPROXIMATION FOR THE DURATION OF THRESHOLD EXCEEDANCE PROBABILITY DENSITY . . . . .	25
REFERENCES . . . . .	37

## FIGURES

1. Axis System (Arrows Indicate Senses of Motions) . . . . .	19
2. Time History of $F_{lat}$ , $\mu_s F_v$ , and $-\mu_s F_v$ . . . . .	19
3. Starboard Sliding Estimator Function Time History . . . . .	20
4. Starboard Sliding Estimator Function Time History . . . . .	20
5. Starboard Sliding Estimator Function Time History . . . . .	21
6. Starboard Sliding Estimator Functions and Thresholds Corresponding to Different Coefficients of Friction . . . . .	21
7. Sliding Estimator Function in Regular Waves . . . . .	22
8. Sliding Estimator Function in Irregular Waves . . . . .	22
9. Definition of Sliding Direction $\delta$ . . . . .	23
10. Illustration of Sliding Calculation for Small $F_{long}$ . . . . .	23
11. Equal-Area Square Approximation to the Circle . . . . .	24
12. Sliding Calculation in the Case of Longitudinal and Lateral Accelerations of Comparable Magnitude . . . . .	24

13. Comparison of Simulated Threshold Exceedance Probability Density Function with Approximations 1 and 2 and the Rayleigh Approximation for a Nondimensional Threshold $r = 0.0$ . . . . .	31
14. Comparison of Simulated Threshold Exceedance Probability Density Function with Approximations 1 and 2 and the Rayleigh Approximation for a Nondimensional Threshold $r = 0.5$ . . . . .	32
15. Comparison of Simulated Threshold Exceedance Probability Density Function with Approximations 1 and 2 and the Rayleigh Approximation for a Nondimensional Threshold $r = 1.0$ . . . . .	33
16. Comparison of Simulated Threshold Exceedance Probability Density Function with Approximations 1 and 2 and the Rayleigh Approximation for a Nondimensional Threshold $r = 1.5$ . . . . .	34
17. Comparison of Simulated Threshold Exceedance Probability Density Function with Approximations 1 and 2 and the Rayleigh Approximation for a Nondimensional Threshold $r = 2.0$ . . . . .	35
18. Comparison of Simulated Threshold Exceedance Probability Density Function with Approximations 1 and 2 and the Rayleigh Approximation for a Nondimensional Threshold $r = 2.5$ . . . . .	36

**TABLES**

	<b>Page</b>
1. Basic Ship Data for the USCG <i>Morganthau</i> . . . . .	6
2. Computed Coefficients of Friction . . . . .	7

<b>Accession For</b>	
NTIS GRA&I	<input checked="" type="checkbox"/>
DTIC TAB	<input type="checkbox"/>
Unannounced	<input type="checkbox"/>
Justification	
By _____	
Distribution/	
Availability Codes	
Dist	Avail and/or Special
A-1	



## NOMENCLATURE

$a$	threshold level
$c$	correlation coefficient, $c = E\{F_{long}S_p\}/\sigma_{long}\sigma_p$
CG	centre of gravity
$\vec{D} = (D_1, D_2, D_3)$	displacements in the three component directions at the point $\vec{P} = (X, Y, Z)$
$E\{F_{long}S_p\}$	expected value of $F_{long}S_p$
erf $y$	error function
$\vec{F}_e$	inertial force in the earth system
$f(F_{long}, S_p)$	joint probability density of $F_{long}, S_p$
$\vec{F}_s$	inertial force in the ship system
$F_{lat}$	lateral force estimator (linearized lateral force per unit mass in the ship system)
$F_{long}$	longitudinal force estimator (linearized longitudinal force per unit mass in the ship system)
$F_{long}/\zeta_0$	transfer function of $F_{long}$
$F_v$	linearized vertical force per unit mass in the ship system
$g$	acceleration due to gravity
$m$	mass
$m_n$	spectral moments of $S_s$
$m_{n, long}$	spectral moments of $F_{long}$
$m_{n, p}$	spectral moments of $S_p$
$m_{n, w}$	spectral moments of $w$
$m_{n, z}$	spectral moments of $z$
$M_p$	number of slides per unit time in the port direction
$M_s$	number of slides per unit time in the starboard direction or, the number of upcrossings by $S_s(t)$ of a threshold at level $a$

$\vec{P} = (X, Y, Z)$	point on the ship
$p_s(\tau)$	duration of threshold exceedance probability density
$r$	nondimensional threshold, $r = a/\sqrt{m_0}$
$S_a(t)$	aft sliding estimator function
$S_f(t)$	forward sliding estimator function
$S_p(t)$	port sliding estimator function
$S_{p,0}/\zeta_0$	transfer function of the port sliding estimator function
$S_{S_s}(\omega_e)$	spectrum of $S_s(t)$
$S_s(t)$	starboard sliding estimator function, assumed to be a zero-mean Gaussian process
$S_{s0}$	amplitude of the starboard sliding estimator function
$t$	time
$T_2$	zero-crossing period, $T_2 = 2\pi\sqrt{m_0/m_2}$
$T_m$	modal period
$t_s$	time at which an object stops sliding
$t^*$	time at which the sliding estimator function crosses the threshold $a$
$x_s$	distance in the starboard direction
$w$	$-F_{long} \sin \epsilon + S_p \cos \epsilon$
$z$	$F_{long} \cos \epsilon + S_p \sin \epsilon$
$\delta$	angle of azimuth defined in Fig. 9
$\epsilon$	rotation angle, $\epsilon = -0.5 \arctan[2c\sigma_{long}\sigma_p/(\sigma_p^2 - \sigma_{long}^2)]$
$\vec{\eta} = (\eta_1, \eta_2, \eta_3)$	translatory displacements of the ship's CG
$\mu_d$	dynamic coefficient of friction
$\mu_s$	static coefficient of friction
$\vec{\xi} = (\xi_4, \xi_5, \xi_6)$	angular displacements of the ship

- $\sigma_{long}$  standard deviation of  $F_{long}(t)$
- $\sigma_p$  standard deviation of  $S_p(t)$
- $\sigma_s$  standard deviation of  $S_s(t)$
- $\tau$  duration of a threshold exceedance
- $\bar{\tau}$  average duration of a threshold exceedance
- $\phi_m$  mean heel angle
- $\phi(r) = (1/\sqrt{2\pi}) \int_r^\infty e^{-x^2/2} dx$
- $\omega$  angular frequency
- $\omega_2$  frequency corresponding to the zero-crossing period,  $T_2$
- $\omega_e$  encounter frequency

## ABSTRACT

*A frequency-domain method of predicting the incidence of personnel or equipment sliding is presented which includes the (linearized) forces due to roll, pitch, longitudinal, lateral and vertical accelerations, and also the effects of non-zero mean heel. The predictions of the method are compared with the results of observations of at-sea sliding incidents, and good correspondence is obtained.*

*A simple approximation for the duration of threshold exceedance probability density is described, and used to develop a method for predicting the incidence of slides greater than a certain severity. The method applies for arbitrary lateral and vertical acceleration, but only to the case in which the longitudinal acceleration is negligible. An example of the application of the method is presented.*

*It is argued that ship motions such as roll, pitch, lateral and longitudinal accelerations are the wrong physical parameters for expressing seakeeping criteria. These criteria become simpler when expressed in terms of the incidence of degrading events such as helicopters sliding, and are equally applicable to all vessel types.*

## ADMINISTRATIVE INFORMATION

This work was done while the first author was on exchange at the David Taylor Research Center from Defence Research Establishment Atlantic. It was sponsored by the Chief of Naval Research, Office of Naval Technology, Code ONT211, under 6.2 Surface Ship Technology Program (ND1A), Program Element 62121N, Advanced Hull Project RH21S23, Task 5, Ship Motion Control. The work was performed during FY1991 under work unit number 1-1506-122. The DN number is DN178067.

## INTRODUCTION

Predictions of the operational performance of ships at sea require three elements: a statistical description of the wave and wind environment in which the ship will operate; computer programs for determining the ship response; and seakeeping criteria to indicate the effects of the motions on operational performance. Hindcast data bases are now available for many operational areas (see e.g. Reference 1), and strip theory computer programs such as SMP<sup>2,3</sup> are in wide-spread use. There has been comparatively less effort devoted to developing seakeeping criteria, and the accuracy of operability predictions is now limited by the accuracy of available criteria.

A summary of criteria in use in 1989 was presented in Reference 4. As an example, criteria for personnel consist of separate limits for each of the following four parameters: roll, pitch, and lateral and vertical acceleration at the pilot house. There are some problems associated with this approach. First, operations are not limited by any one of these

parameters individually, but rather by some combination of all four. A value of roll which will cause extreme problems in the presence of significant vertical accelerations, will be perfectly acceptable when vertical motions are small. Second, the criteria are primarily based on operational experience with frigates and destroyers. While the limiting values of these parameters found do reflect the level of motions at which significant personnel problems occur on these vessels, they may result in misleading predictions of the operability of SWATH vessels or even of monohulls of significantly different size. For example, the pitch criterion of  $1.5^\circ$  RMS which is based on operational experience on vessels with length to beam ratios of about 9 with most frequently occurring pitch periods of around 6 seconds might be conservative if applied to a SWATH vessel with a length to beam ratio of 2 and longer pitch periods.

In fact, roll, pitch, vertical and lateral accelerations are the wrong physical parameters for expressing personnel criteria. The limiting values of these parameters found through operational experience are representative of the motion levels at which certain degrading effects start to become important. For personnel operating on deck, the degrading effects are the onset of loss-of-balance events due to tipping or sliding. These events were called motion-induced interruptions (MII) in Reference 5. Reference 6 introduced a frequency-domain method for predicting the incidence of motion-induced interruptions that included the effects of both lateral and vertical acceleration, and proposed that a rational seakeeping criterion for deck operations involving personnel could be developed in terms of the incidence of MII's per unit time.

In future, we propose that all seakeeping criteria should be presented in terms of limits on the incidence of whatever degrading event is determined to limit the operation of interest rather than the underlying ship motions. As an example, we consider an unsecured helicopter on deck, as addressed in Reference 7. In this case, the degrading event of most interest is the onset of helicopter sliding. A criterion in terms of the maximum acceptable number of slides per hour is physically easy to understand, and obviously applies equally to SWATH or monohull vessels. The alternative approach of trying to determine separate limits for the contributing motions of roll, pitch, vertical, lateral, and longitudinal accelerations as well as relative wind will not lead to a unique answer because of their interrelation; moreover, different values will be obtained depending on whether the deck is slippery or not. If, on the other hand, the criterion is expressed in terms of a limit on the allowable number of slides per unit time, the effect of the coefficient of friction is automatically taken into account. It should be noted that the philosophy outlined above is already used routinely for slamming and deck wetness criteria which are usually expressed as limits on the number of slams or wetnesses per hour.

In order to implement our approach to developing seakeeping criteria, two steps are required. First methods must be developed to predict the incidence and severity of degrading events such as sliding of helicopters or MII's of personnel on deck. In order to lead to practical tools for ship design, these methods must work in the frequency

domain. Second, operational data are required to determine acceptable limits for the incidence of occurrence of the degrading events.

In this report, which is an extension of Reference 6, we present a frequency-domain method of predicting the incidence and severity of personnel or equipment sliding which includes the (linearized) forces due to roll, pitch, longitudinal, lateral and vertical accelerations, and also the effects of non-zero mean heel angle. An analysis of personnel tipping which includes the above forces and also steady and unsteady wind effects will be published later\*.

### PREDICTION OF SLIDING INCIDENCE WITH ZERO LONGITUDINAL ACCELERATION

In this section, we review the frequency-domain method for predicting sliding incidence in the absence of longitudinal acceleration which was presented in Reference 6. Longitudinal acceleration is usually negligible for large monohulls, but need not be for small monohulls or different platform types. A method for predicting sliding incidence in the presence of combined longitudinal, lateral, and vertical acceleration will be presented in a later section.

Two coordinate systems will be used for the sliding calculations. The inertial system is illustrated in Fig. 1. Its origin is located at the mean position of the ship and it translates with the mean velocity of the ship, maintaining a fixed orientation with respect to the free surface. The motions surge, sway, heave, roll, pitch, yaw will be denoted by  $\eta_i$ ,  $i = 1, \dots, 6$ .

The displacement  $\vec{D} = (D_1, D_2, D_3)$ , at a point  $\vec{P} = (X, Y, Z)$  on the ship is given by

$$\vec{D} = \vec{\eta} + \vec{\xi} \times \vec{P} \quad (1)$$

where  $\vec{\eta} = (\eta_1, \eta_2, \eta_3)$  and  $\vec{\xi} = (\xi_1, \xi_2, \xi_3)$ . For example, the displacement in the vertical direction is given by

$$D_3 = \eta_3 + \eta_4 Y - \eta_5 X \quad (2)$$

and includes contributions from heave, roll, and pitch. The velocities and accelerations at  $\vec{P}$  are obtained by differentiating Eq. 1 with respect to time.

$$\dot{\vec{D}} = \dot{\vec{\eta}} + \dot{\vec{\xi}} \times \vec{P} \quad (3)$$

$$\ddot{\vec{D}} = \ddot{\vec{\eta}} + \ddot{\vec{\xi}} \times \vec{P} \quad (4)$$

---

\*Graham, R., Baitis, A.E., and Meyers, W.G., "On the Development of Operability Criteria", to appear in *Naval Engineers Journal*, ASNE Day, 1992

An object of mass  $m$  fixed to the ship with center of gravity located at the point  $\bar{P}$  experiences an inertial force, which in the earth system is given by

$$\vec{F}_e = -m(\ddot{D}_1, \ddot{D}_2, \ddot{D}_3 + g) \quad (5)$$

where  $g$  is the acceleration due to gravity. The object could be an unsecured helicopter on deck, a crew member, or anything else. For the development of seakeeping criteria, the forces perpendicular and parallel to the deck are of more relevance. These are the forces in the ship reference system,  $\vec{F}_s$ .

Fig. 1 also illustrates the ship coordinate system, which is now fixed to the ship. Performing the coordinate transformation from the earth to ship reference system, and retaining only the linear terms we obtain

$$\vec{F}_s = m(-\ddot{D}_1 + g\eta_5, -\ddot{D}_2 - g\eta_4, -\ddot{D}_3 - g) \equiv m(F_{long}, F_{lat}, F_v) \quad (6)$$

The quantities  $F_{long}$  and  $F_{lat}$  are the (linearized) longitudinal and lateral forces per unit mass, and following Reference 5 will be called the longitudinal and lateral force estimators.  $F_v$  is the (linearized) vertical force per unit mass.

Suppose that the object under consideration has a static coefficient of friction given by  $\mu_s$ . Under the assumption that  $F_{long} \approx 0$ , slides can only occur in the port or starboard directions. A slide to port will occur whenever

$$mF_{lat} > -m\mu_s F_v \quad (7)$$

or

$$-\ddot{D}_2 - g\eta_4 - \mu_s \ddot{D}_3 > \mu_s g \quad (8)$$

On the other hand, the object will slide to starboard if

$$mF_{lat} < m\mu_s F_v \quad (9)$$

or

$$\ddot{D}_2 + g\eta_4 - \mu_s \ddot{D}_3 > \mu_s g \quad (10)$$

The quantities on the left hand sides of Eqs. 8 and 10 were called generalized lateral force estimators in Reference 6. In the present work, these quantities will be called sliding estimator functions, and denoted by  $S_p$  and  $S_s$ , respectively.

Wind forces on the ship or asymmetric loading conditions may result in the presence of a steady heel angle,  $\phi_m$  (positive starboard side down). In this case, the right hand sides of Eqs. 8 and 10 should be replaced by  $\mu_s g + \phi_m g$  and  $\mu_s g - \phi_m g$ , respectively. The net result is to make sliding more likely to occur in the downhill direction.

In Reference 6, a frequency-domain method was derived for predicting the number of slides per unit time, under the assumption that the sliding estimator functions followed

the Rayleigh distribution. In fact, the result holds provided that  $S_p(t)$  and  $S_s(t)$  are zero-mean Gaussian processes, and is not restricted to narrow-band processes. Let  $S_{S_s}(\omega_e)$  denote the (one-sided) power spectral density of  $S_s(t)$  as a function of encounter frequency  $\omega_e$ , and denote by  $m_n$  the spectral moments of  $S_{S_s}(\omega_e)$ .

$$m_n = \int_0^{\infty} \omega_e^n S_{S_s}(\omega_e) d\omega_e \quad (11)$$

Rice<sup>8</sup> (see also Reference 9) showed that the number of upcrossings (or downcrossings) per unit time of a threshold at level  $a$  is given by

$$M_s = \frac{1}{2\pi} \sqrt{\frac{m_2}{m_0}} \exp\left(-\frac{a^2}{2m_0}\right) \quad (12)$$

The quantity  $M_s$  is the number of slides per unit time in the starboard direction. In the absence of steady heel, the threshold  $a$  is at  $\mu_s g$ . In the general case, the threshold  $a$  is at  $\mu_s g - \phi_m g$ . The number of slides in the port direction  $M_p$  can be estimated in a similar manner.

The onset of widespread sliding of objects on board ship is indicative of a level of motion which makes all shipboard operations difficult, and necessitates tying down all moveable objects. It is suggested that a minimal seakeeping criterion for almost any operation is that the probability of sliding remain acceptably low.

The probability of sliding depends on the precise location on the ship; hence, in specifying a sliding criterion, it is also necessary to specify a location or series of locations of interest. For a transit mission, for example, the locations of interest could be the bridge, the engine room, etc., and the sliding criterion would have to be evaluated simultaneously at the various locations. The incidence and severity of sliding which is considered tolerable at each location will ultimately have to depend on the tasks being performed and the degree of degradation in task performance which sliding causes. Normally, this degradation will result from the reduced pace of task performance, but in some cases, e.g. aircraft sliding on deck, sliding may result in injuries to personnel or damage to equipment.

### COMPARISON OF MEASURED AND PREDICTED SLIDING INCIDENCE

In order to validate the method presented above for predicting sliding incidence, the results of a chair-sliding experiment conducted in 1989 on board the USCG *Morganthau* were analysed. Unlike helicopter sliding, chair sliding is more likely to be a nuisance than to result in serious degradation of operational performance; however, the chair sliding experiment described here provides a valid check of the method, and had the advantage of being easy to conduct without appreciable danger to the crew or equipment. Moreover, the lower coefficients of friction on the inside of the ship allow this

type of experiment to be conducted under much less severe conditions than would be necessary to cause an appreciable incidence of helicopter sliding events.

Basic ship data for the *Morganthau* are given in Table 1. In this experiment, a subject sitting in a standard government issue chair with metal feet was located in a compartment with a linoleum floor which had been pitted and scarred from heavy use. The subject was facing to port and was located in front of a computer terminal. At the onset of the chair sliding, the subject was instructed to press a function key which time-stamped the data. A total of 25 slides were recorded during the course of the experiment, which lasted 20 minutes. The ship was heeled to starboard by 3.3 degrees, and as a consequence, all of the slides occurred in this direction.

Table 1. Basic Ship Data for the USCG *Morganthau*

Displacement	3055.	tonnes
LBP	106.7	metres
Beam	12.80	metres
Draft	4.40	metres

The chair was located about 1.5 metres to port of the centreline and 2.0 metres aft of the ship's centre of gravity. The ship motion instrumentation, which was installed for an unrelated experiment, was located near the flight deck at a centreline position 26.9 metres aft of the CG. The flight deck lateral and vertical accelerations were corrected to the position of the chair, by using the measured roll, pitch and yaw signals to take into account the difference in moment arms. The longitudinal acceleration at the chair was estimated using the recorded pitch signal and the distance of the chair from the waterline and it was found to be negligible.

From Eqs. 7 and 9, slides should occur whenever  $F_{lat} > -\mu_s F_v$  or  $F_{lat} < \mu_s F_v$ . Unfortunately, the coefficient of friction of the chair on the floor was not measured directly during the experiment, but estimates were obtained by computing the values of the ratio  $|F_{lat}|/|F_v|$  for the observed sliding incidents. The values obtained are shown in Table 2.

In practice, only 17 of the 25 sliding incidents were included in Table 2, since it appeared that the subject was slow in time-stamping the remaining slides. Motion data was recorded at three samples per second, and so, the uncertainty in the starting time of the slides was probably about 0.5 seconds. The values shown in Table 2 result in a mean coefficient of friction of 0.189 with a standard deviation of 0.024. The variation in the  $\mu_s$  values found is consistent with the poor condition of the floor. It should be noted that even under laboratory conditions, significant variation in coefficients of friction are found when measurements are repeated. (See for example Reference 10.)

Figure 2 illustrates a sample plot of  $F_{lat}$ ,  $\mu_s F_v$ , and  $-\mu_s F_v$  versus time. From Eqs. 7 and 9, slides should occur whenever  $F_{lat}$  crosses either of the other two curves. The time

Table 2. Computed Coefficients of Friction

Time of Event	$\mu_s$	Time of Event	$\mu_s$
34.9	.184	967.3	.191
54.6	.182	1038.9	.219
75.5	.205	1117.2	.207
302.6	.174	1125.8	.175
500.1	.174	1141.8	.176
559.7	.166	1152.5	.211
776.8	.168	1176.1	.211
803.8	.162	1186.1	.245
827.1	.161		

stamps corresponding to the recorded slides are shown as vertical lines on the figure.

The same information can be presented in terms of the starboard sliding estimator function, which, from Eq. 10, is given by  $S_s = -F_{lat} - \mu_s \ddot{D}_3$ . In this context,  $F_{lat}$  is simply minus the lateral acceleration at the chair since the acceleration was measured in the ship reference system and therefore already includes the component of gravity parallel to the deck due to the roll angle. The mean offset in  $F_{lat}$  due to the nonzero heel angle should be removed, so that the upcrossings of  $S_s$  can be estimated using Eq. 12, which is only applicable to zero-mean processes. Slides are predicted to occur whenever  $S_s$  exceeds the threshold  $\mu_s g - g\phi_m$ . Figure 3 shows a plot of the starboard sliding estimator function for the same time interval as shown in Fig. 2. The threshold  $\mu_s g - g\phi_m$  is also shown in the figure. Although Figs. 2 and 3 contain the same information, the presentation of Fig. 3 results in a constant threshold, and allows the sliding incidence to be estimated in the frequency domain.

Figures 4 and 5 show plots of the sliding estimator function for two other time slices. Good correspondence between observed sliding incidents and threshold crossings is obtained in Fig. 4, except for the fifth slide, which appears to have been noted late, and the eighth slide, which seems to occur at an anomalously low  $S_s$  value. The experimenter noted that the slides at the end of this time slice were rather large. This is in qualitative agreement with the large threshold exceedances which occurred during the sixth and seventh slides.

On the other hand, the correspondence between threshold crossings and observed slides shown in Fig. 5 is poor. In this case, the two events shown do not correspond to threshold crossings, while a subsequent crossing did not result in an event. Figure 6 presents the same time slice, with the addition of the starboard sliding estimator functions and thresholds corresponding to coefficients of friction of plus or minus one standard deviation about the mean. The effect of the change in coefficient of friction on the sliding estimators is small; however, the effect on the threshold is significant.

The two events shown now correspond to crossings of the lower threshold, while the 'non-event' at 882 seconds did not exceed the upper threshold. Effectively, the variation in the coefficient of friction results in uncertainty as to whether a particular crossing will result in an event. For the purposes of validating the method presented herein, it is most important that the average number of events be predicted correctly.

Overall, the correspondence between threshold crossings and observed sliding events was as follows. Sixteen of the observed slides corresponded to threshold crossings, whereas nine events did not. On the other hand, there were seven upcrossings which did not result in events for a total of twenty-three upcrossings. This corresponds well with the observed number of twenty-five slides. The number of upcrossings was also estimated using Eq. 12 and the computed standard deviations of the sliding estimator function and its time derivative. This resulted in an estimate of 24.5 upcrossings for the twenty minute period which is also in close correspondence with the observed number of slides.

It should be noted that real data may show significant variability in the number of upcrossings in adjacent time slices. It must be emphasized that the method presented here is statistical, and only determines the average number of upcrossings over a sufficiently long period.

### PREDICTION OF SLIDING SEVERITY WITH ZERO LONGITUDINAL ACCELERATION

For some applications, notably fixed-wing operations on aircraft carriers, operators routinely tolerate numerous small sliding incidents, and only curtail operations when severe slides start to occur. This suggests that it may be of interest to predict not only the onset of sliding, but also to predict the severity of sliding, as measured by the distance that the object slides before coming to rest. The purpose of this section is to present an approximate frequency-domain method for estimating the probability of occurrence of sliding incidents of arbitrary severity. The method only applies to the case in which the longitudinal acceleration can be neglected.

#### REGULAR WAVE CASE

In this section, we treat the special case in which the starboard (or port) sliding estimator function is sinusoidal, and we first assume that the dynamic coefficient of friction,  $\mu_d$ , and the static coefficient of friction,  $\mu_s$ , are equal. In this case

$$S_s(t) = S_{s0} \sin \omega t \tag{13}$$

and the situation is as illustrated in Fig. 7. We denote by  $t^*$  the time at which

$$S_{s0} \sin \omega t^* = a \tag{14}$$

where  $a = \mu_s g - \phi_m g$ . Choosing  $t = t^*$  as the new time origin, the mass experiences a force given by

$$m(S_{s0} \sin \omega(t + t^*) - ag) \quad \text{for } t \geq t^* \quad (15)$$

Denoting the distance in the starboard direction by  $x_s$ , we have

$$m\ddot{x}_s(t) = m(S_{s0} \sin \omega(t + t^*) - ag) \quad (16)$$

The velocity at time  $t$  is given by

$$\dot{x}_s(t) = \left[ \frac{\sqrt{S_{s0}^2 - a^2}}{\omega} (1 - \cos \omega t) + \frac{a}{\omega} \sin \omega t - at \right] \quad (17)$$

for times  $t \geq t^*$  such that  $\dot{x}_s(t)$  is greater than zero. Once the mass comes to rest, the frictional force keeps it at rest until the next threshold exceedance. Eq. 17 can be solved iteratively to determine the time  $t_s$  at which the mass stops. Choosing our origin at the initial rest position of the object, the distance at time  $t$  is given by

$$x_s(t) = \left[ \frac{\sqrt{S_{s0}^2 - a^2}}{\omega} \left( t - \frac{\sin \omega t}{\omega} \right) + \frac{a}{\omega^2} (1 - \cos \omega t) - \frac{1}{2} at^2 \right] \quad (18)$$

The distance travelled can now be determined by substituting  $t = t_s$  in the previous equation.

In the case  $\mu_d \neq \mu_s$ , the force per unit mass on the object after the onset of sliding in the starboard direction becomes

$$-F_{lat} - \mu_d \ddot{D}_3 - \mu_d g + \phi_m g \quad (19)$$

when the sliding estimator function exceeds the threshold  $(\mu_s - \phi_m)g$ . Equation 19 will be approximated by

$$-F_{lat} - \mu_s \ddot{D}_3 - (\mu_d - \phi_m)g = S_s(t) - (\mu_d - \phi_m)g \quad (20)$$

This approximation is required because of the method used to estimate the amplitude of the sliding estimator functions in the frequency domain which will be discussed in the next section. It can be expected to be good whenever the vertical acceleration is small compared to  $g$ , or when  $\mu_s - \mu_d$  is small.

With the approximation of Eq 20, and a sinusoidal sliding estimator function, the velocity and distance travelled in the starboard direction become

$$\dot{x}_s(t) = \left[ \frac{\sqrt{S_{s0}^2 - a^2}}{\omega} (1 - \cos \omega t) + \frac{a}{\omega} \sin \omega t - (\mu_d - \phi_m)gt \right] \quad (21)$$

$$x_s(t) = \left[ \frac{\sqrt{S_{s0}^2 - a^2}}{\omega} \left( t - \frac{\sin \omega t}{\omega} \right) + \frac{a}{\omega^2} (1 - \cos \omega t) - \frac{1}{2} (\mu_d - \phi_m)gt^2 \right] \quad (22)$$

While the incidence of sliding depends only on  $\mu_s$ , the sliding distance depends mainly on  $\mu_d$  which determines the magnitude of the frictional force once motion has started. As an example, for an angular frequency of 0.628 (corresponding to a ten-second period for the sliding estimator function), an amplitude of 0.5  $g$ 's, and zero heel angle, Eq. 22 predicts a sliding distance of 0.57 metres for  $\mu_s = 0.45 = \mu_d$ , but a sliding distance of 4.36 metres for  $\mu_s = 0.45$  and  $\mu_d = 0.35$ . Another consequence of Eq. 22 is that if there is a large difference between  $\mu_s$  and  $\mu_d$ , there are no insignificant slides: all slides are serious ones.

## IRREGULAR WAVE CASE

A time history of the starboard sliding estimator function derived from the chair sliding experiment is shown in Fig. 8. We will assume that in the vicinity of a threshold exceedance the sliding estimator function can be adequately approximated by a sine wave. It remains to develop frequency-domain methods for estimating the amplitude and angular frequency of typical threshold exceedances.

We will make use of a high-threshold approximation for the duration of exceedance probability density function due to Rice<sup>11</sup>. In Appendix A, the applicability of this approximation to the wave elevation process is investigated, and is shown to give good results for thresholds greater than or equal to one standard deviation. This condition is not unduly restrictive for present purposes, since if the standard deviation of the sliding estimator function is greater than or equal to the sliding threshold, it is clear that severe sliding is so common that operations would be impossible.

As before, we assume that the sliding estimator function  $S_s(t)$  is a zero-mean, Gaussian, stochastic process (not necessarily narrow-banded), and suppose that the threshold level is at  $a$ . We define the nondimensional threshold by  $r = a/\sigma_s$ , where  $\sigma_s \equiv \sqrt{m_0}$  is the standard deviation of  $S_s(t)$ .

We will denote by  $\tau$  the duration of a given threshold exceedance, and the duration probability density by  $p_s(\tau)$ . From Eq. 61 of Appendix A, we have the following approximation for the duration probability density  $p_s(\tau)$

$$p_s(\tau) \approx \frac{\pi M_s^2}{2[\phi(\tau)]^2} \tau \exp\left(-\frac{\pi M_s^2}{4[\phi(\tau)]^2} \tau^2\right) \quad (23)$$

where  $\phi(\tau)$  is defined in Eq. 56.

With the sine wave approximation, the duration of exceedance of a threshold can be used to determine the amplitude of the sliding estimator function, provided that the angular frequency is known. We assume that the angular frequency can be adequately approximated by the frequency  $\omega_2$  corresponding to the zero-crossing period  $T_2$ , as illustrated in Fig. 8. The accuracy of this assumption will be briefly discussed below. We have

$$T_2 = 2\pi \sqrt{\frac{m_0}{m_2}} \quad (24)$$

For a sinusoidal exceedance of the threshold  $a$  of duration  $\tau$  with frequency  $\omega_2$ , the amplitude  $S_{s0}$  is given by

$$S_{s0} = \frac{a\sqrt{2(1 - \cos \omega_2 \tau)}}{\sin \omega_2 \tau} \quad (25)$$

As before, the threshold for the starboard sliding estimator function is given by  $\mu_s - \phi_m g$ .

Putting these results together, we have the following numerical procedure for estimating the probability of occurrence of slides of distance greater than an arbitrary length  $l$ . We determine the amplitude of the sliding estimator function  $S'_{s0}$  which results in a slide of distance  $l$  by solving Eq. 22 iteratively. The duration  $\tau^l$  resulting in this amplitude is obtained by solving Eq. 25

$$\tau^l = \frac{1}{\omega_2} \arccos \left[ 2 \left( \frac{a}{S'_{s0}} \right)^2 - 1 \right] \quad (26)$$

The fraction of threshold crossings that result in slides of distance greater than  $l$  is given by

$$\int_{\tau^l}^{\infty} p_s(\tau) d\tau = \exp \left( -\frac{\pi M_s^2}{4[\phi(\tau)]^2} (\tau^l)^2 \right) \quad (27)$$

The number of slides per second of distance greater than  $l$  is obtained by multiplying Eq. 27 by  $M_s$ , which is given in Eq. 12.

As an example of an application of the method, we will revisit the chair-sliding experiment considered above and compute the expected number of slides of distance greater than 1.8 metres (6 feet) in a twenty minute period. No estimates of the dynamic coefficient of friction were available, but for the purposes of the exercise,  $\mu_d$  was assumed to be 0.15. As before, the sliding threshold was at  $\mu_s g - \phi_m g = 0.131g$ . For this experiment,  $\omega_2 = 0.679$ , and it was found that a sliding estimator amplitude of 0.149  $g$ 's resulted in a sliding distance of 1.8 metres. The corresponding duration of exceedance from Eq. 26 was 1.47 seconds. From Eq. 27, the fraction of slides of distance greater than 1.8 metres was found to be 0.54, so that the expected number of slides of distance greater than 1.8 metres in a twenty minute period was  $24.5 \times 0.54 = 13.2$ .

In order to get some idea of the accuracy of using the zero-crossing frequency  $\omega_2$  in determining the amplitudes corresponding to a threshold exceedance of given duration, the threshold crossings of the chair sliding experiment were analyzed. For each crossing, the duration and amplitude of the sliding estimator function were measured, and the corresponding frequency  $\omega_2$  was determined from Eq. 26. The resulting estimates of  $\omega_2$  had a mean value of 0.61 and a standard deviation of 0.12. This compares with an  $\omega_2$  value of 0.68 computed from Eq. 24. This suggests that Eq. 25 may be sufficiently accurate for practical purposes, but further investigation is required.

## PREDICTION OF SLIDING INCIDENCE WITH NONZERO LONGITUDINAL ACCELERATION

In this section, we present a frequency-domain method for predicting the incidence of sliding in the presence of combined vertical, lateral, and longitudinal acceleration. We first present an accurate method which is restricted to longitudinal accelerations that are small compared with the lateral acceleration, which is the case of most interest on monohull vessels. We then present an approximate method for dealing with the case of comparable longitudinal and lateral accelerations.

We first consider the case of zero heel angle. A slide will occur in some direction whenever

$$\sqrt{F_{long}^2 + F_{lat}^2} > \mu_0(g + \ddot{D}_3) \quad (28)$$

or

$$\sqrt{F_{long}^2 + F_{lat}^2} - \mu_0 \ddot{D}_3 > \mu_0 g \quad (29)$$

Under the assumption that  $F_{long}$  and  $F_{lat}$  are jointly Gaussian, it can be shown that  $\sqrt{F_{long}^2 + F_{lat}^2}$  follows the Rayleigh distribution. Unfortunately, the distribution of  $\sqrt{F_{long}^2 + F_{lat}^2} - \mu_0 \ddot{D}_3$  is the convolution of a Rayleigh distribution with a Gaussian distribution, and is not tractable. It is therefore necessary to develop approximate solutions.

We first consider the case in which the longitudinal acceleration is small compared with the lateral acceleration. Suppose that at a given instant in time the resultant force parallel to the deck (the vector sum of  $F_{lat}$  and  $F_{long}$ ) is in the direction  $\delta$  shown in Fig. 9. The resultant force will result in a slide in this direction provided that

$$F_{long} \cos \delta + F_{lat} \sin \delta - \mu_0 \ddot{D}_3 > \mu_0 g \quad (30)$$

Under the assumption that  $F_{long}$  is small (but not necessarily negligible) compared with  $F_{lat}$ , most of the sliding incidents will take place within some range about  $\delta = 90^\circ$  and  $\delta = 270^\circ$ , and slides near  $\delta = 0^\circ$  and  $\delta = 180^\circ$  will be very unlikely.

We will estimate the number of slides to port by determining the incidence of up-crossings of  $\mu_0 g$  by the resultant of  $F_{long}$  and  $S_p \equiv F_{lat} - \mu_0 \ddot{D}_3$  for which  $\delta$  is in the neighbourhood of  $90^\circ$ . The resultant of  $F_{long}$  and  $S_p$  is in the direction  $\delta^* \equiv \arctan(F_{lat} - \mu_0 \ddot{D}_3)/F_{long}$  and has magnitude

$$F_{long} \cos \delta^* + F_{lat} \sin \delta^* - \mu_0 \ddot{D}_3 \sin \delta^* \quad (31)$$

whereas the direction of the resultant force parallel to the deck is given by  $\delta \equiv \arctan(F_{lat}/F_{long})$  and the condition for sliding in the direction  $\delta$  is given by Eq. 30. We will approximate  $\delta$  by  $\delta^*$ , and approximate the sliding condition by

$$F_{long} \cos \delta^* + F_{lat} \sin \delta^* - \mu_s \ddot{D}_3 \sin \delta^* > \mu_s g \quad (32)$$

A preliminary assessment of the accuracy of this approximation was made by examining recorded acceleration time histories from the T-AGOS monohull. Equations 30 and 32 were both evaluated in the time domain, and the resulting predictions of the total number of sliding incidents were compared. From these results, it appears that Equation 32 provides a good approximation to Equation 30 provided that the RMS longitudinal acceleration is less than about half of the RMS lateral acceleration.

As an aside, we note that the method presented here for small longitudinal acceleration would apply for arbitrary longitudinal acceleration if the vertical acceleration were zero. For monohulls, it is difficult to conceive of a situation in which this combination would occur.

We assume that  $F_{long}$  and  $S_p$  are jointly Gaussian with zero means, standard deviations  $\sigma_{long}$  and  $\sigma_p$ , respectively, and correlation coefficient  $c = E\{F_{long}S_p\}/\sigma_{long}\sigma_p$ , where  $E\{F_{long}S_p\}$  denotes the expected value of  $F_{long}S_p$ . Under these assumptions their joint probability density,  $f(F_{long}, S_p)$  is given by

$$f(F_{long}, S_p) = \frac{1}{2\pi\sigma_{long}\sigma_p\sqrt{1-c^2}} e^{-\frac{1}{2(1-c^2)} \left[ \frac{F_{long}^2}{\sigma_{long}^2} - \frac{2cF_{long}S_p}{\sigma_{long}\sigma_p} + \frac{S_p^2}{\sigma_p^2} \right]} \quad (33)$$

Although  $F_{long}$  and  $S_p$  are not independent, we can apply a coordinate rotation  $\epsilon$  to obtain independent random variables

$$\begin{pmatrix} z \\ w \end{pmatrix} = \begin{pmatrix} F_{long} \cos \epsilon + S_p \sin \epsilon \\ -F_{long} \sin \epsilon + S_p \cos \epsilon \end{pmatrix} \quad (34)$$

provided that  $\epsilon$  is given by

$$\tan 2\epsilon = -\frac{2c\sigma_{long}\sigma_p}{\sigma_p^2 - \sigma_{long}^2} \quad (35)$$

We will estimate the number of slides near  $\delta = 90^\circ$  as the number of upcrossings of the threshold  $\mu_s g$  by the resultant of  $z$  and  $w$  in the half plane  $w > 0$ . Slides for which  $\delta$  is not in the neighbourhood of  $90^\circ$  will be rare unless  $\sigma_{long}$  is a significant fraction of  $\mu_s g$ , and in this case  $\sigma_p$  will be sufficiently large to cause wide-spread sliding anyway.

As shown in Fig. 10, the number of slides that occur at a distance  $z = z_0$  from the  $w$  axis can be estimated as the sum of the number of  $w$  up-crossings of the level  $\sqrt{(\mu_s g)^2 - z_0^2}$  which occur in the small interval  $dz_0$  about  $z_0$  plus the number of  $z$  up-crossings of the level  $z_0$  which occur in the small interval  $dw_0$  about  $\sqrt{(\mu_s g)^2 - z_0^2}$ . An estimate of the total number of slides to port,  $M_p$ , is obtained by integrating over  $z_0$ . Denoting the  $i$ th spectral moments of  $z$  and  $w$  by  $m_{i,z}$  and  $m_{i,w}$  respectively, and

making use of the independence of these two random variables, we obtain

$$\begin{aligned}
M_p &= \int_{-\mu g}^{\mu g} \frac{1}{2\pi} \sqrt{\frac{m_{2,w}}{m_{0,w}}} e^{-\frac{(\mu g)^2}{2m_{0,w}} + \frac{z_0^2}{2m_{0,w}}} \frac{1}{\sqrt{2\pi m_{0,z}}} e^{-\frac{z_0^2}{2m_{0,z}}} dz_0 + \\
&\int_{-\mu g}^{\mu g} \frac{1}{2\pi} \sqrt{\frac{m_{2,z}}{m_{0,z}}} e^{-\frac{z_0^2}{2m_{0,z}}} \frac{1}{\sqrt{2\pi m_{0,w}}} e^{-\frac{(\mu g)^2}{2m_{0,w}} + \frac{z_0^2}{2m_{0,w}}} \frac{z_0 dz_0}{\sqrt{(\mu g)^2 - z_0^2}} \\
&= \frac{1}{2\pi} \sqrt{\frac{m_{2,w}}{m_{0,w}}} e^{-\frac{(\mu g)^2}{2m_{0,w}}} \frac{1}{\sqrt{1 - (m_{0,z}/m_{0,w})}} \operatorname{erf}(\sqrt{b}) + \\
&\frac{1}{2\pi} \sqrt{\frac{m_{2,z}}{m_{0,z}}} e^{-\frac{(\mu g)^2}{2m_{0,w}}} \frac{\sqrt{2\mu g}}{\sqrt{\pi m_{0,w}}} \int_0^1 e^{-by^2} \frac{y dy}{\sqrt{1-y^2}}
\end{aligned} \tag{36}$$

where

$$b = \frac{(\mu g)^2}{2} \left( \frac{1}{m_{0,z}} - \frac{1}{m_{0,w}} \right) \tag{37}$$

and 'erf' denotes the error function, which is defined in Eq. 58 of Appendix A. The integral over  $y$  in Eq. 36 appears to be improper; however, making the substitution  $x^2 = 1 - y^2$  we obtain

$$\int_0^1 e^{-by^2} \frac{y dy}{\sqrt{1-y^2}} = \int_0^1 e^{-b(1-x^2)} dx \tag{38}$$

In general, this last integral can be evaluated numerically; however, in the case that  $b$  is large, most of the contribution to the integral over  $y$  in Eq. 36 will come from the points near the origin. In this case, the integral can be estimated by expanding  $1/\sqrt{1-y^2}$  about  $y = 0$ . We obtain

$$\int_0^1 e^{-by^2} \frac{y dy}{\sqrt{1-y^2}} \approx \frac{1}{2b} + \frac{1}{4b^2} - e^{-b} \left[ \frac{3}{4b} + \frac{1}{4b^2} \right] \tag{39}$$

The spectral moments of  $z$  and  $w$  can be expressed in terms of the moments and cross-spectral moments of  $F_{long}$  and  $S_p$ . Let  $(F_{long,0}/\zeta_0)$  and  $(S_{p,0}/\zeta_0)$  denote the (complex) transfer functions of  $F_{long}$  and  $S_p$ , respectively, and  $S_\zeta(\omega_e)$  denote the wave spectrum as a function of encounter frequency  $\omega_e$ .

$$m_{0,z} = \int_0^\infty \left( \frac{\overline{F_{long,0}}}{\zeta_0} \cos \epsilon + \frac{\overline{S_{p,0}}}{\zeta_0} \sin \epsilon \right) \left( \frac{F_{long,0}}{\zeta_0} \cos \epsilon + \frac{S_{p,0}}{\zeta_0} \sin \epsilon \right) S_\zeta(\omega_e) d\omega_e \tag{40}$$

where the bars indicate complex conjugates. We have

$$\begin{aligned}
m_{0,z} &= \sigma_{long}^2 \cos^2 \epsilon + 2E\{F_{long} S_p\} \sin \epsilon \cos \epsilon + \sigma_p^2 \sin^2 \epsilon \\
&= \sigma_{long}^2 \cos^2 \epsilon + 2c\sigma_{long}\sigma_p \sin \epsilon \cos \epsilon + \sigma_p^2 \sin^2 \epsilon
\end{aligned} \tag{41}$$

Making use of Eq. 35, we obtain

$$m_{0,z} = \frac{1}{2}(\sigma_{long}^2 + \sigma_p^2) - \frac{1}{2}\sqrt{(\sigma_p^2 - \sigma_{long}^2)^2 + (2c\sigma_{long}\sigma_p)^2} \quad (42)$$

Similarly,

$$m_{0,w} = \frac{1}{2}(\sigma_{long}^2 + \sigma_p^2) + \frac{1}{2}\sqrt{(\sigma_p^2 - \sigma_{long}^2)^2 + (2c\sigma_{long}\sigma_p)^2} \quad (43)$$

The second moments can be determined in an analogous fashion. If we denote by  $I$  the integral

$$I \equiv \int_0^\infty \omega_e^2 \left( \frac{F_{long,0} S_{p,0}}{\zeta_0} + \frac{F_{long,0} S_{p,0}}{\zeta_0} \right) S_\zeta(\omega_e) d\omega_e \quad (44)$$

we obtain

$$m_{2,z} = \frac{1}{2}(m_{2,long} + m_{2,p}) - \frac{(m_{2,p} - m_{2,long})(\sigma_p^2 - \sigma_{long}^2)}{2\sqrt{(\sigma_p^2 - \sigma_{long}^2)^2 + (2c\sigma_{long}\sigma_p)^2}} - \frac{Ic\sigma_{long}\sigma_p}{\sqrt{(\sigma_p^2 - \sigma_{long}^2)^2 + (2c\sigma_{long}\sigma_p)^2}} \quad (45)$$

and

$$m_{2,w} = \frac{1}{2}(m_{2,long} + m_{2,p}) + \frac{(m_{2,p} - m_{2,long})(\sigma_p^2 - \sigma_{long}^2)}{2\sqrt{(\sigma_p^2 - \sigma_{long}^2)^2 + (2c\sigma_{long}\sigma_p)^2}} + \frac{Ic\sigma_{long}\sigma_p}{\sqrt{(\sigma_p^2 - \sigma_{long}^2)^2 + (2c\sigma_{long}\sigma_p)^2}} \quad (46)$$

The incidence of sliding in the starboard direction can be determined in a similar fashion. In the presence of a mean heel angle  $\phi_m$  the threshold  $\mu_0 g$  should be replaced by  $\mu_0 + \phi_m g$  and  $\mu_0 - \phi_m g$ , for port and starboard sliding, respectively.

To gain some insight into the increased sliding incidence which results from the presence of nonzero longitudinal acceleration, we will compare the port sliding incidence predicted from Eq. 36 with the sliding incidence from Eq. 12 for a numerical example. We assume  $\sigma_{long} = \sigma_p/3$  and  $\sigma_p/3 = 0.5\mu_0 g$ ,  $c = 0.5$ , and  $\phi_m = 0$ . For simplicity, we take

$$(1/2\pi)\sqrt{m_{2,p}/m_{0,p}} = (1/2\pi)\sqrt{m_{2,w}/m_{0,w}} = (1/2\pi)\sqrt{m_{2,z}/m_{0,z}} \quad (47)$$

For this example, we find that the presence of longitudinal acceleration increases the sliding incidence by about 14%.

For longitudinal acceleration larger than about half the lateral acceleration, it is no longer reasonable to assume that all of the slides will occur near the port and starboard directions. An estimate of the number of sliding incidents in the case of comparable lateral and longitudinal accelerations can be obtained as follows. The coefficient of

friction  $\mu_s$  is the same at all angles of azimuth; hence, a polar plot  $\mu_s$  as a function of  $\delta$  forms a circle. We will (somewhat crudely) approximate this circle by a square of equal area, as shown in Fig. 11. The coefficient of friction now becomes a function of  $\delta$ . Suppose that at a given instant, the resultant force parallel to the deck is in the direction  $\delta$  as shown in Fig. 12. The condition for sliding in the direction  $\delta$  which was given in Eq. 30 now becomes

$$F_{long} \cos \delta + F_{lat} \sin \delta - \mu_s(\delta) \ddot{D}_3 > \mu_s(\delta) g \quad (48)$$

Note however, that in order for a slide to occur in some direction  $\delta$  in the quadrant within  $45^\circ$  of the longitudinal direction, it is necessary and sufficient that

$$F_{long} - \mu_s(0) \ddot{D}_3 > \mu_s(0) g \quad (49)$$

To see this, we note that Eq. 48 is equivalent to

$$\sqrt{F_{long}^2 + F_{lat}^2} - \mu_s(\delta) \ddot{D}_3 > \mu_s(\delta) g \quad (50)$$

Multiplying this result by  $\cos \delta = F_{long} / \sqrt{F_{long}^2 + F_{lat}^2}$  we obtain

$$F_{long} - \mu_s(\delta) \cos \delta \ddot{D}_3 > \mu_s(\delta) \cos \delta g \quad (51)$$

which is equivalent to Equation 49.

If we define the forward sliding estimator function as

$$S_f = F_{long} - \mu_s(0) \ddot{D}_3 \quad (52)$$

then the forward slides can be estimated by counting the upcrossings of  $S_f$  of the threshold  $\mu_s(0)g$ . Similarly, we define the aft sliding estimator function via

$$S_a = -F_{long} - \mu_s(0) \ddot{D}_3 \quad (53)$$

The total number of slides can be approximated by summing the upcrossings of the sliding estimator functions in the four primary directions. For the equal area square approximation to the circle, we have  $\mu_s(0) = \mu_s \sqrt{\pi}/2 = 0.886\mu_s$ .

The reader is cautioned that in the case of small longitudinal acceleration, this approximation results in an overestimate of the number of slides. For the example considered above in which  $\sigma_{long} = \sigma_p/3$  and  $\sigma_p/3 = 0.5\mu_s g$ , the number of sliding incidents predicted to occur to port with the reduced threshold  $0.886\mu_s$  is 54% larger than the sliding incidence with the original threshold. The more careful analysis presented above showed that the presence of longitudinal acceleration produced an increase of only 14%. The estimates obtained with the square approximation should improve in the case of comparable longitudinal and lateral accelerations.

## CONCLUDING REMARKS

A frequency-domain method of predicting the incidence of personnel or equipment sliding has been presented. The method includes the (linearized) forces due to roll, pitch, longitudinal, lateral and vertical accelerations, and also the effects of non-zero mean heel. Two different solutions were developed according to the relative size of the longitudinal acceleration. The method developed for small longitudinal acceleration is accurate, while the method developed for comparable longitudinal and lateral accelerations is more approximate, but should still produce estimates of sufficient accuracy for practical purposes. The predictions of the method were compared with the results of a chair-sliding experiment conducted at sea, and good correspondence was obtained.

A simple approximation for the duration of threshold exceedance probability density was described, and used to develop a method for predicting the incidence of slides greater than a certain severity. The method applies for arbitrary lateral and vertical acceleration, but only to the case in which the longitudinal acceleration is negligible. An example of the application of the method was presented.

It has been proposed that in future, seakeeping criteria should be presented in terms of the tolerable incidence of degrading events such as helicopter sliding. Criteria in this form are simple and are equally applicable to all vessel types.

## ACKNOWLEDGEMENTS

The authors would like to thank Mr. J.F. Dalzell for valuable discussions. Dr. Graham would like to acknowledge the hospitality of the David Taylor Research Center during the writing of this paper.

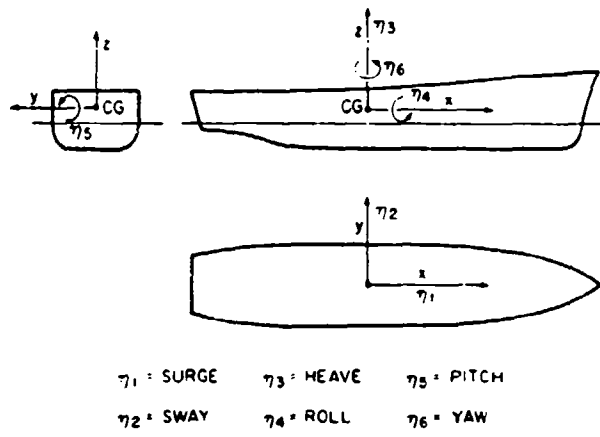


Fig. 1. Axis System (Arrows Indicate Senses of Motions)

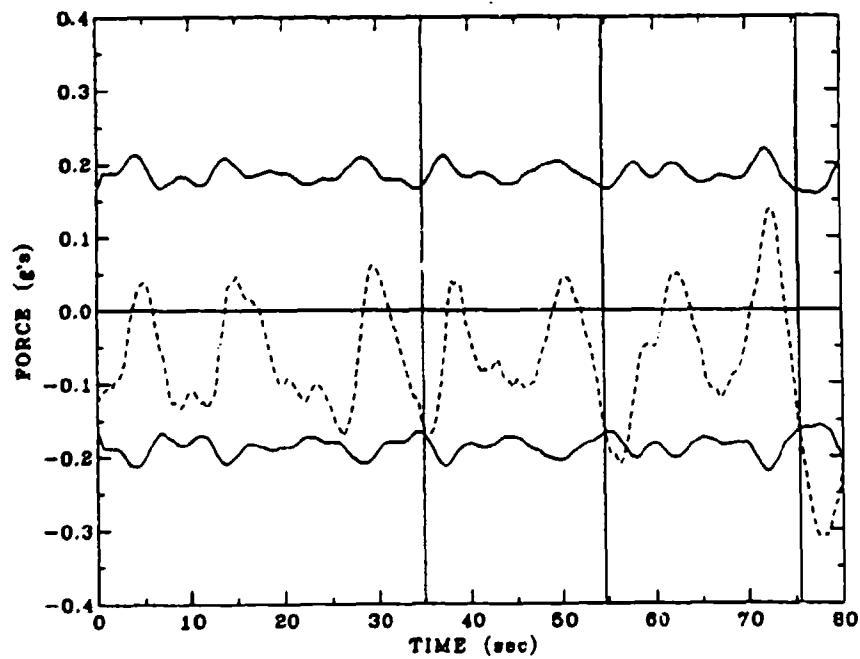


Fig. 2. Time History of  $F_{lat}$ ,  $\mu_v F_v$ , and  $-\mu_v F_v$ .

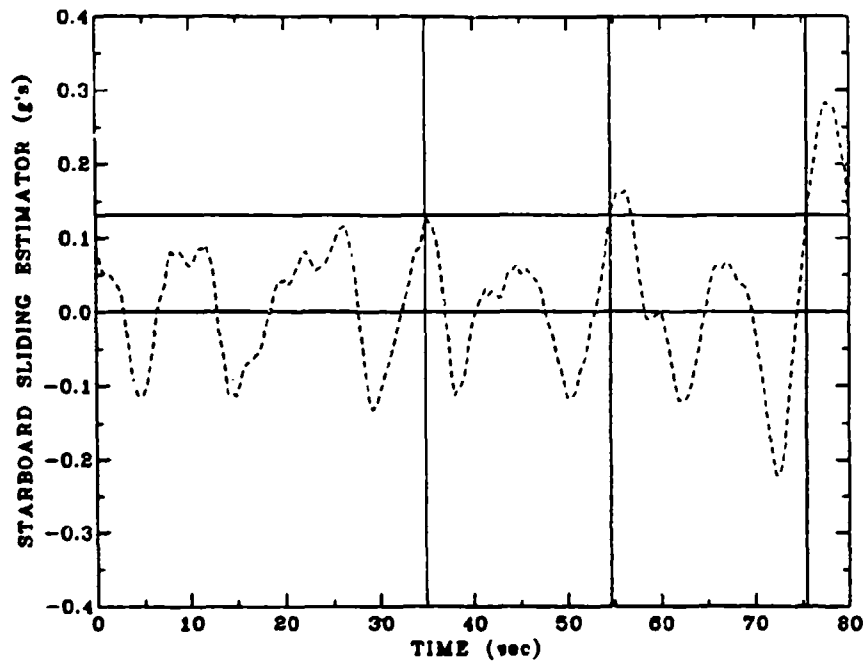


Fig. 3. Starboard Sliding Estimator Function Time History

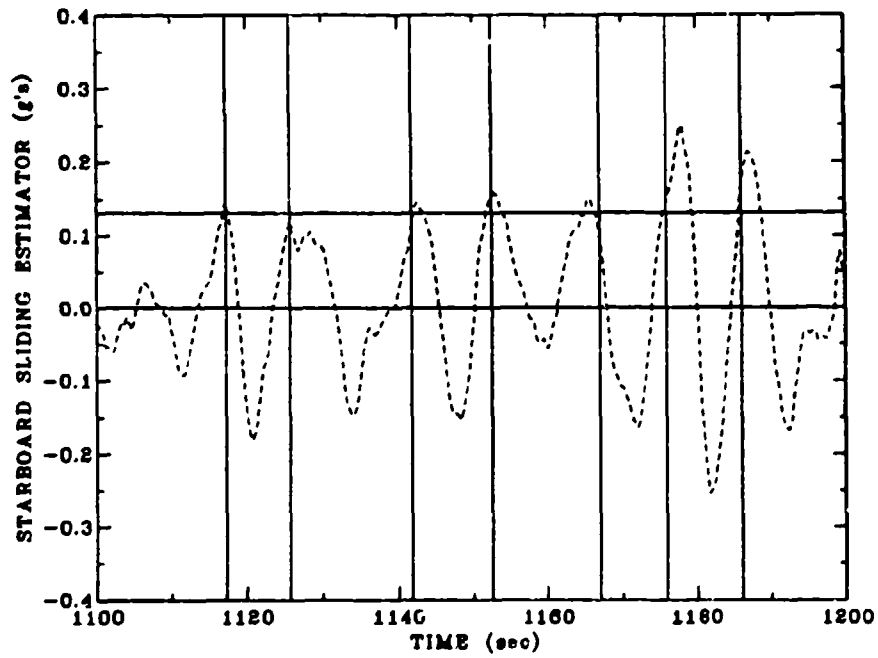


Fig. 4. Starboard Sliding Estimator Function Time History

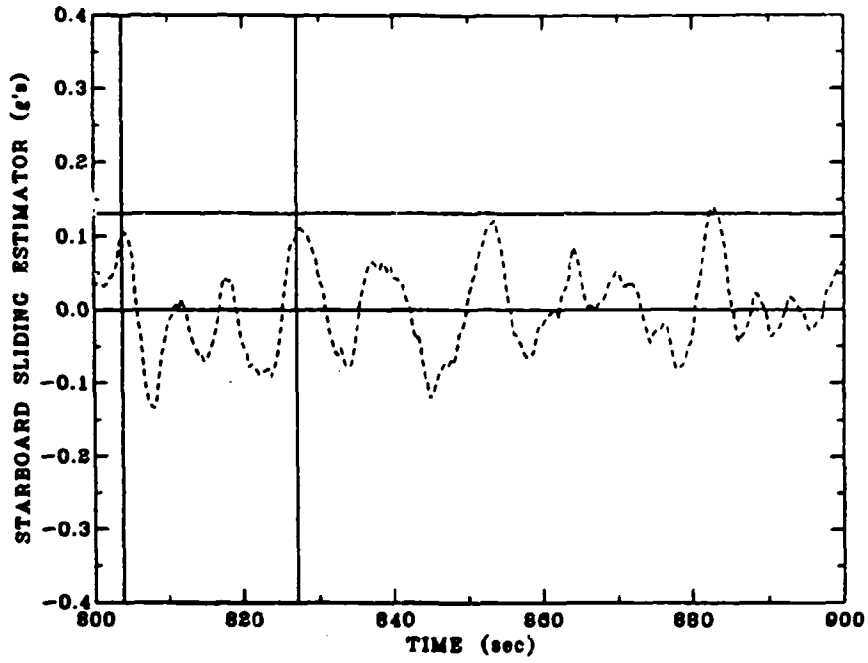


Fig. 5. Starboard Sliding Estimator Function Time History

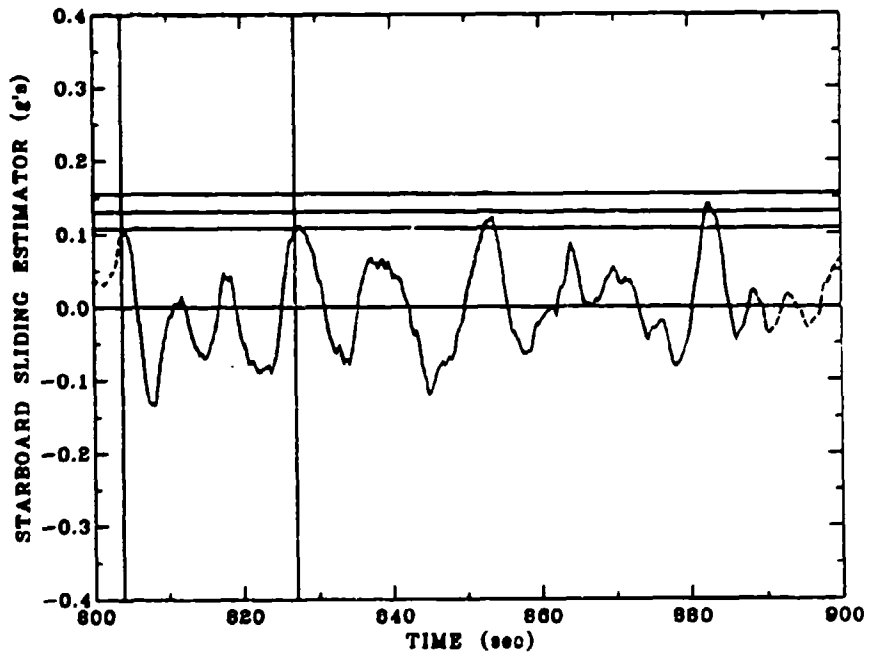


Fig. 6. Starboard Sliding Estimator Functions and Thresholds Corresponding to Different Coefficients of Friction

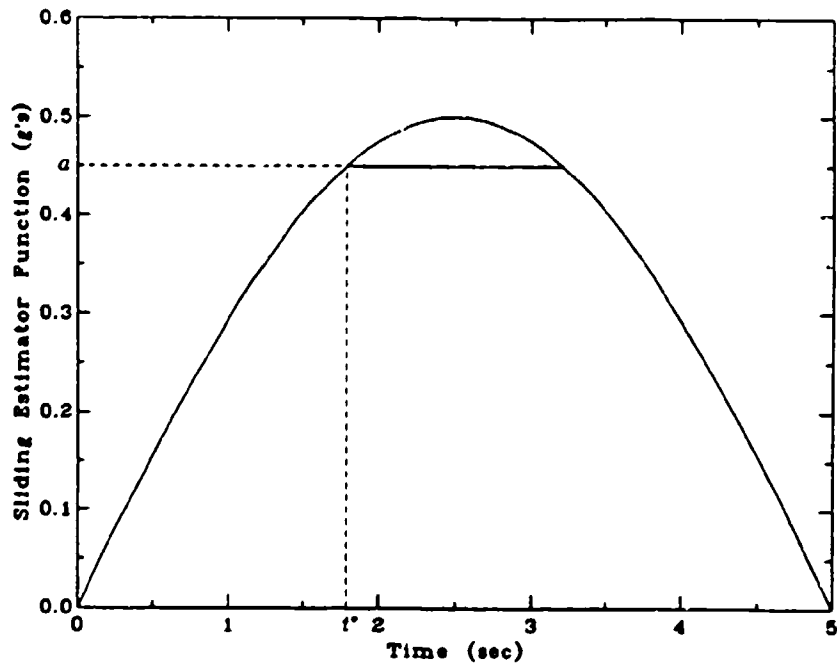


Fig. 7. Sliding Estimator Function in Regular Waves

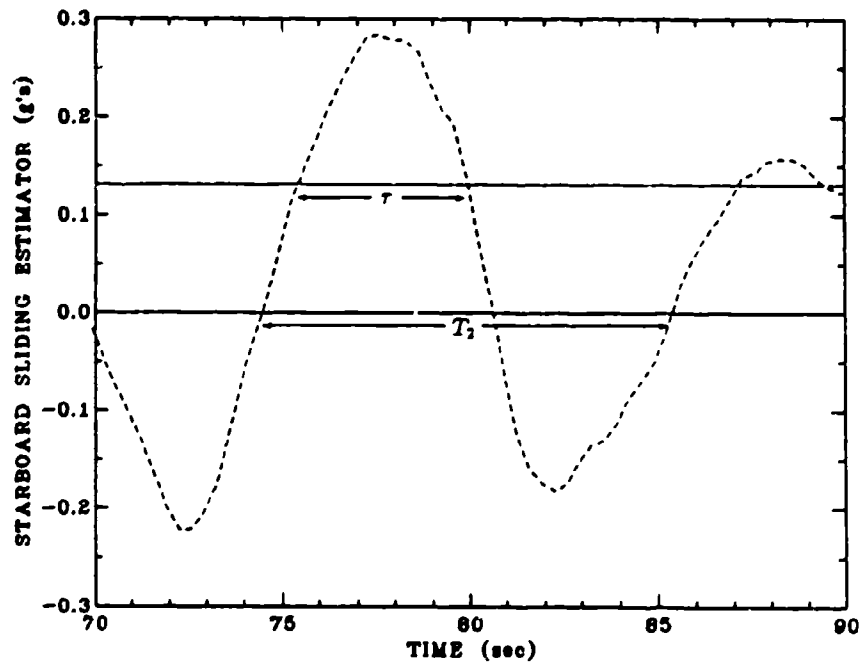


Fig. 8. Sliding Estimator Function in Irregular Waves

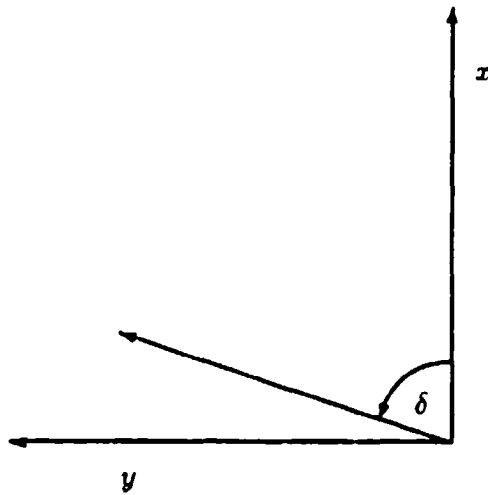


Fig. 9. Definition of Sliding Direction  $\delta$

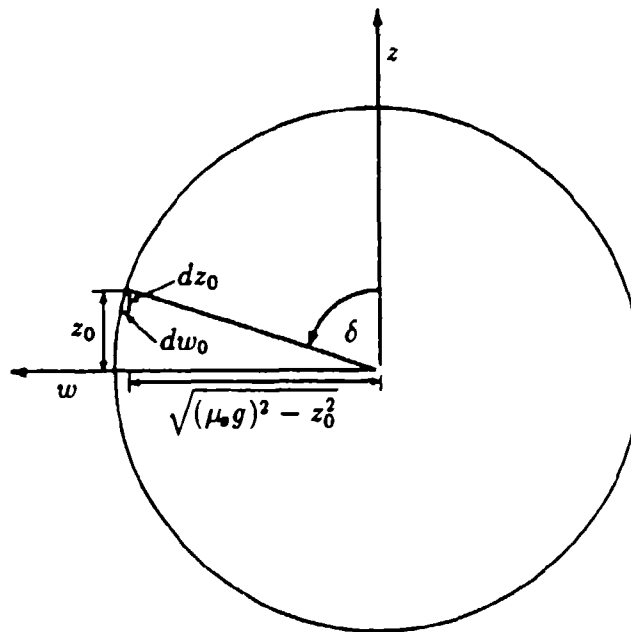


Fig. 10. Illustration of Sliding Calculation for Small  $F_{long}$

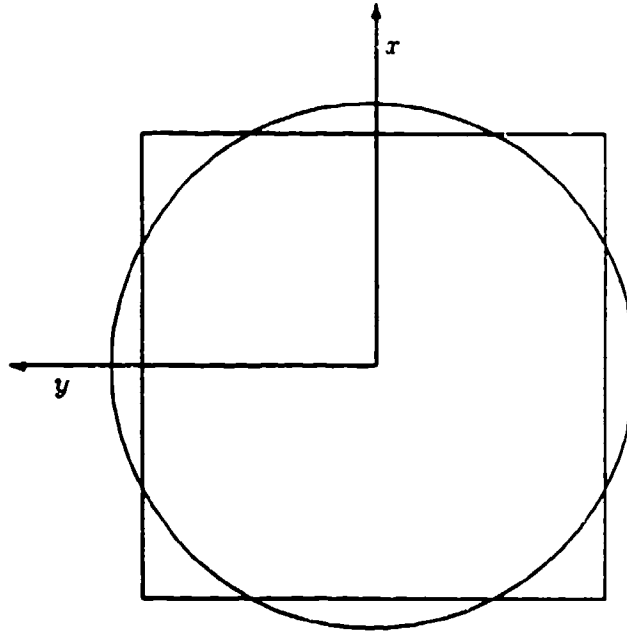


Fig. 11. Equal-Area Square Approximation to the Circle.

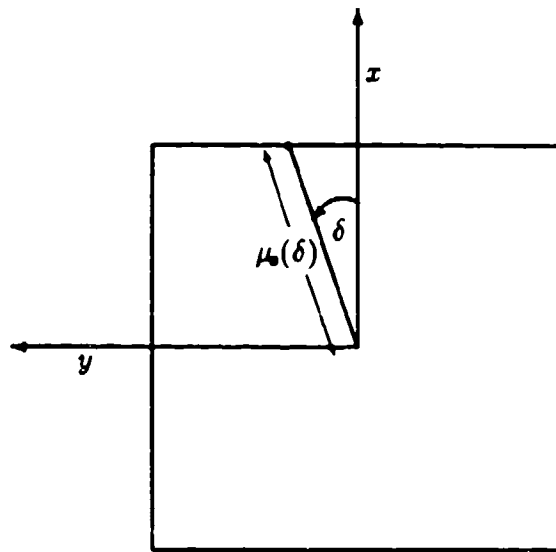


Fig. 12. Sliding Calculation in the Case of Longitudinal and Lateral Accelerations of Comparable Magnitude

APPENDIX A  
A SIMPLE APPROXIMATION FOR THE DURATION  
OF THRESHOLD EXCEEDANCE PROBABILITY DENSITY

by  
Ross Graham and John F. Dalzell

**INTRODUCTION**

In seakeeping research, there are frequent occasions when the number of up-crossings of a threshold by a zero-mean, Gaussian stochastic process must be determined. Standard examples include estimating the probability of keel emergence and the probability of deck wetness. The solution to this problem is well-known, and was first developed by Rice<sup>8</sup> (see also Price and Bishop<sup>9</sup>).

For certain applications, information on the duration of time that the process spends above the threshold is also required. Complete information on the duration statistics would be provided by the duration of exceedance probability density, but unfortunately, this density can only be estimated numerically, and the available approximations are both difficult to implement, and suffer from serious problems.

The first of the available approximations originates with the theory of Rice<sup>11</sup>, as refined by Kuznetsov, Stratanovich and Tikhonov<sup>12,13</sup>. (The theory and approximations are also partially described by Price and Bishop<sup>9</sup>.) The "exact" theory deals with the conditional probability density for the duration of exceedance of an arbitrary threshold, with no pre-conditions about the nature of the process or the statistical independence of the times of threshold crossings. The conditioning of the density is upon the value of the threshold, with a duration event defined as the time interval between successive up- and down-crossings of the threshold. This "exact" theory takes the form of an infinite functional series which was impossible to evaluate in the 1960's—and probably still is. Hence, practical use has involved approximations and assumptions of one sort or another.

The boldest simplifying assumption is that *all* the times of threshold crossings are statistically independent. With this assumption, the durations become a Poisson process, a model which appears relevant for very high thresholds, and which has been noted in the seakeeping literature<sup>14</sup>.

The usual approach for arbitrary thresholds is due to Rice<sup>11</sup> and Tikhonov<sup>13</sup>, and will be called "Approximation 1" herein. This approximation involves taking only the first term of the infinite series of the exact theory as an approximation for arbitrary threshold levels but "small" durations. Unfortunately, this approach yields a result which is not exactly that desired. In effect, the approximate density involves the probabilities that, given a threshold up-crossing at some time,  $t_0$ , there is a down-crossing threshold in the neighborhood of a later time  $t$ , *regardless* of what happened between time  $t_0$  and  $t_0 + t$ . As a result, Approximation 1 appears to yield good approximations to the true density

for short durations, but does not integrate to unity, and in fact the integral may not even be finite.

An essentially more modern treatment of the problem is due to Rainal<sup>15</sup> and Mikami<sup>16,17</sup>. In these works, the estimation of the conditional density was formulated in a different way, and by making the assumption that a given individual interval between threshold crossings is statistically independent of nearly all the possible sums of preceding intervals, the problem was reduced to the solution of a Volterra integral equation involving the numerical results from Approximation 1, described above. On the whole, Approximation 2, though more computer intensive, yields more satisfying results than Approximation 1. However, the approximation has disquieting faults of its own—principally that the computed density may become negative for large durations.

Thus, *both* of the available approximations for arbitrary threshold levels are useless when moments of the density are required. The purpose of this appendix is to examine a high-threshold approximation which was developed in Reference 11, but which appears to have gone unnoticed. The approximation, which is described in the next section, has a simple analytic form and satisfies the basic requirements of a probability density. The question of how high the threshold must be before a good approximation is obtained is investigated in a later section using the results of a time domain simulation of a typical long-crested wave system.

### APPROXIMATION FOR THE DURATION OF THRESHOLD EXCEEDANCE PROBABILITY DENSITY

Let  $S_s(t)$  be a zero-mean, Gaussian, stochastic process (not necessarily narrow-banded). In the main text,  $S_s(t)$  is assumed to be the starboard sliding estimator function, but is an arbitrary function in this appendix. Let  $\sigma_s$  denote the standard deviation of  $S_s(t)$ , and suppose that the threshold level is at  $a$ . We define the nondimensional threshold by  $\tau = a/\sigma_s$ .

We will denote by  $\tau$  the duration of a given threshold exceedance, and the duration probability density by  $p_s(\tau)$ . Rice<sup>11</sup> demonstrates that for high thresholds,  $p_s(\tau)$  tends towards the Rayleigh probability density, i.e.

$$p_s(\tau) \rightarrow \lambda \tau e^{-\lambda \tau^2/2} \quad (54)$$

Rice (see also Vanmarcke<sup>18</sup>) shows that the average duration  $\bar{\tau}$  of a threshold exceedance is given by

$$\bar{\tau} = \frac{\phi(\tau)}{M_s} \quad (55)$$

where  $M_s$  is given in Eq. 12, and

$$\phi(\tau) \equiv \frac{1}{\sqrt{2\pi}} \int_{\tau}^{\infty} e^{-x^2/2} dx \quad (56)$$

Equation 55 is not restricted to high threshold levels. The function  $\phi(r)$  is related to the error function  $\text{erf}(y)$  via

$$\phi(r) = \frac{1}{2} \left[ 1 - \text{erf} \left( \frac{r}{\sqrt{2}} \right) \right] \quad (57)$$

where

$$\text{erf}(y) = \frac{2}{\sqrt{\pi}} \int_0^y e^{-x^2} dx \quad (58)$$

For the Rayleigh probability density, we have

$$\bar{\tau} = \int_0^{\infty} \tau \lambda \tau e^{-\lambda \tau^2/2} d\tau = \sqrt{\frac{\pi}{2\lambda}} \quad (59)$$

so that

$$\lambda = \frac{\pi}{2\bar{\tau}^2} = \frac{\pi M_s^2}{2[\phi(r)]^2} \quad (60)$$

This results in the following approximation<sup>11</sup> for  $p_s(\tau)$

$$p_s(\tau) \approx \frac{\pi M_s^2}{2[\phi(r)]^2} \tau \exp \left( -\frac{\pi M_s^2}{4[\phi(r)]^2} \tau^2 \right) \quad (61)$$

for high enough thresholds.

## TIME DOMAIN SIMULATION

In order to get some feeling for how high a threshold must be in order to obtain reasonable results with the Rayleigh approximation of Eq. 61, a typical long-crested wave system was modeled as a zero-mean Gaussian process, simulated in the time domain, and the resulting "data" used to derive some duration statistics for comparison with the approximation.

Though the results were later nondimensionalized, the variance spectrum of the long-crested wave system was chosen to be of the Bretschneider type with modal period,  $T_m$ , of 9 seconds and significant height of 4 units. The mechanics of the time domain simulation involved the "fast convolution" method in which: pseudo-random bandlimited white noise is Fast Fourier transformed; the resulting transform is modified by a nonrealizable frequency domain filter corresponding to the desired variance spectrum; and an inverse Fast Fourier Transform then in turn yields the simulated process.

The time series simulations of realizations of the selected wave spectrum were generated in "handy-sized" realizations of 8K point time series, at delta-time of 0.1 seconds. Thirty independent realizations of the process were simulated by entering the computer

noise generator at widely separated points in its sequence. Considering all of the samples, the simulation was equivalent to a 6.7 hour observation of the wave process defined by the 9 second modal period spectrum.

A threshold crossing analysis was performed on the simulated data for six nondimensional thresholds corresponding to  $r = 0, 0.5, 1.0, 1.5, 2.0$  and  $2.5$ . The mean time interval between threshold crossings was first computed, and found to agree well with the corresponding theoretical estimates ( $1/M_s$ ), Eq. 12. The computed time differences between each up- and down-crossing were combined into an ordered sample for further analysis, and each duration,  $\tau$ , was nondimensionalized by the wave modal period,  $T_m$ .

For purposes of comparisons with theory, an estimate of the mean probability density over some small interval of duration was required. A uniform nondimensional duration class interval,  $\Delta\{\tau/T_m\}$ , was first assumed and the number of simulated exceedance durations falling into each was tallied. The resulting tallies were divided by the total number of exceedance durations in the sample to form an estimate of the probability,  $[p_s(\tau/T_m) \Delta\{\tau/T_m\}]$ , and then this result was divided by  $\Delta\{\tau/T_m\}$  to form an estimate of the mean probability density over the interval. For graphical purposes these estimates were associated with the mid-point of the nondimensional class interval.

## RESULTS AND DISCUSSION

The results from the simulation are compared with Eq. 61 in Figs. 13 through 18 in terms of the nondimensional duration time  $\tau/T_m$ . Computations of duration densities according to Approximations 1 and 2 as described in the introduction are shown for comparison.

As expected, the comparison is poor for a 0 threshold (Fig. 13), and at most fair for  $r = 0.5$  (Fig. 14), but the results are surprisingly good for the higher threshold levels. The comparison shown in Fig. 15 for  $r = 1.0$  is already quite acceptable, and Figs. 16, 17 and 18 show that good agreement is obtained at higher thresholds.

A closer examination of Figs. 13 to 18 reveals that the average duration  $\bar{\tau}$  of a threshold exceedance is slightly underestimated in all cases. In theory, Eq. 55 should hold exactly for all threshold levels. The discrepancy appears to arise from differences in the theoretical estimate of  $m_2$  in Eq. 12, and the value of  $m_2$  realized in the simulated time history. The theoretical estimate was obtained by direct integration of the analytical expression for the Bretschneider spectrum, and is slightly higher than the  $m_2$  value for the simulation. This discussion serves to highlight that accurate estimates of the threshold exceedance probability density depend strongly on accurate estimates of  $m_2$ .

It is concluded that, at least for the sample wave elevation process considered here, Eq. 61 provides a reasonable engineering approximation to the threshold exceedance duration probability density function for nondimensional thresholds greater than or equal to one.

It should be noted that the wave elevation process is narrow-banded. The applica-

bility of the Rayleigh approximation for the exceedance duration probability density of wide-band processes requires further investigation.

### **CONCLUDING REMARKS**

A simple approximation due to Rice<sup>11</sup> for the duration of threshold exceedance probability density at high threshold levels was presented, and its applicability to the wave elevation process was investigated, by comparison with the results of a time-domain simulation. Unlike other more complicated approximations in use, this approximation has a simple analytic form, namely, the Rayleigh probability density.

It was found that the simple approximation compared well with the time-domain simulation results for nondimensional thresholds greater than or equal to one.

$r = 0.0$ , 3603 Simulated Events

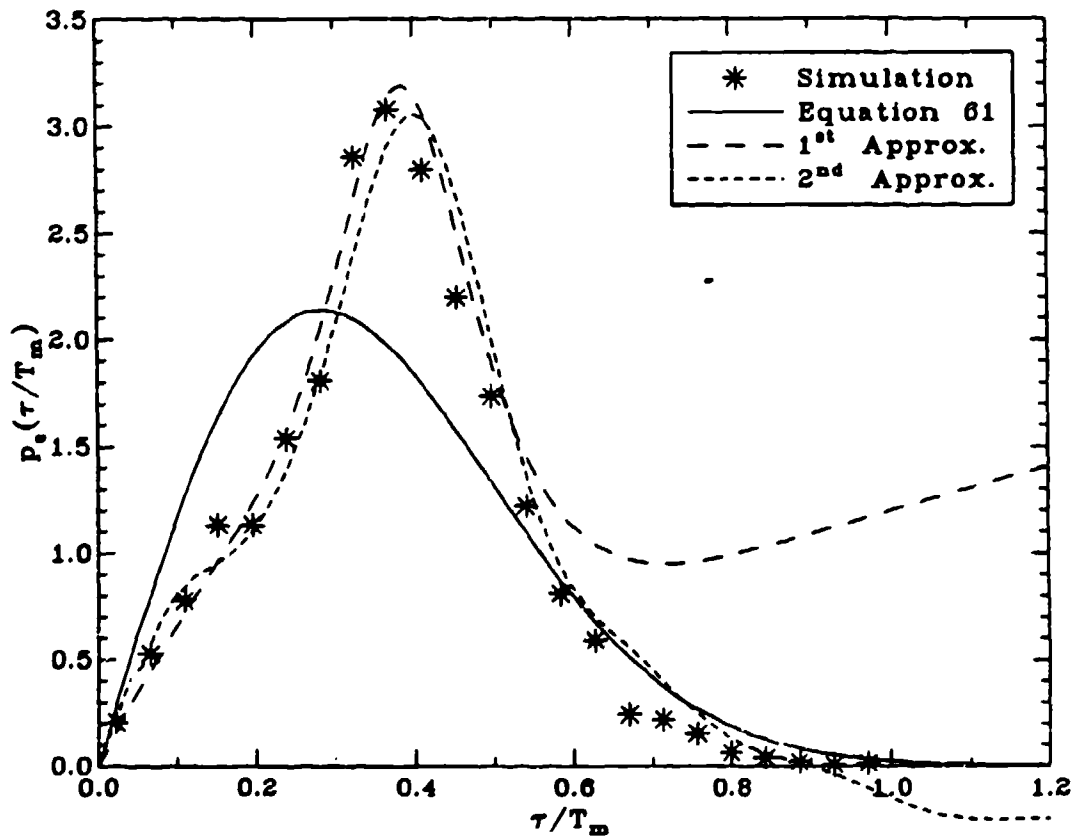


Fig. 13. Comparison of Simulated Threshold Exceedance Probability Density Function with Approximations 1 and 2 and the Rayleigh Approximation for a Nondimensional Threshold  $r = 0.0$

$r = 0.5$ , 3206 Simulated Events

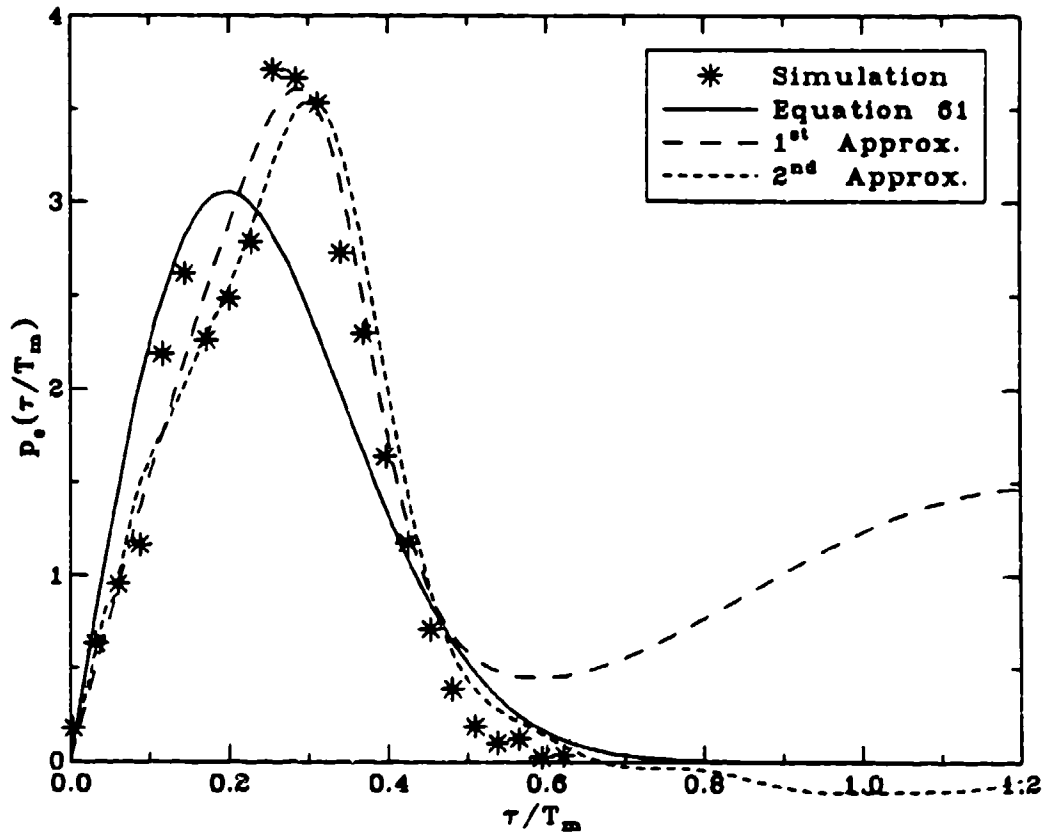


Fig. 14. Comparison of Simulated Threshold Exceedance Probability Density Function with Approximations 1 and 2 and the Rayleigh Approximation for a Nondimensional Threshold  $r = 0.5$

$r = 1.0$ , 2236 Simulated Events

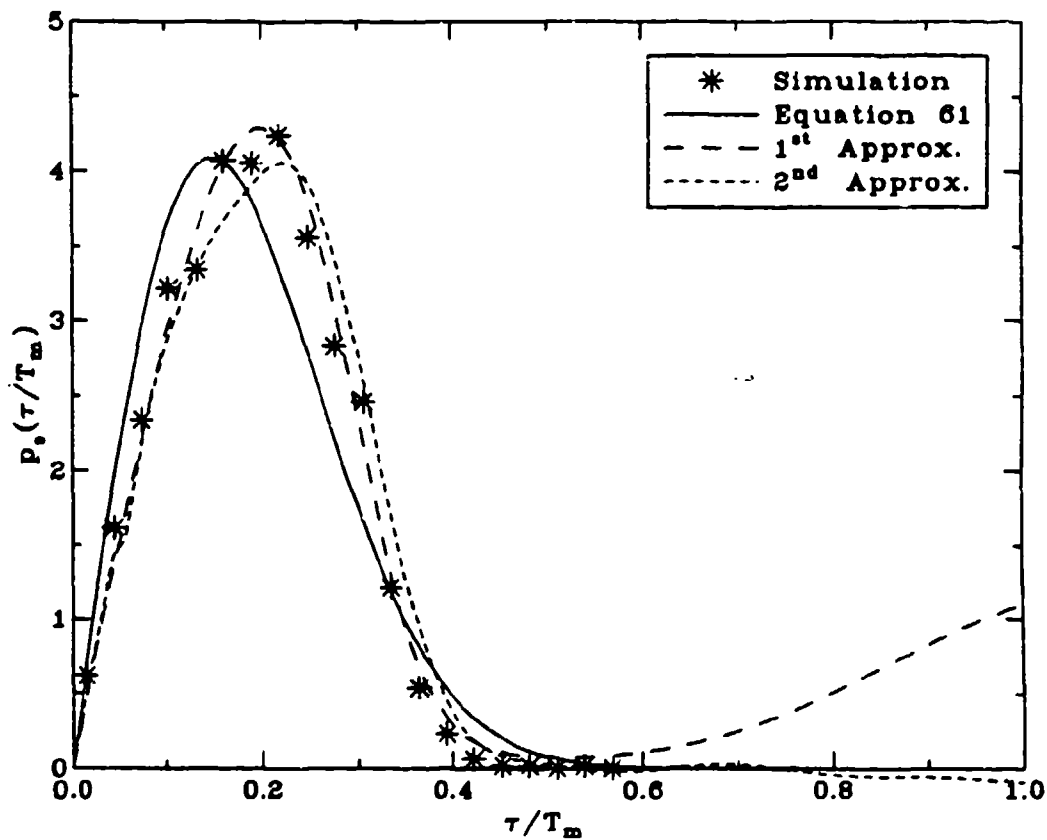


Fig. 15. Comparison of Simulated Threshold Exceedance Probability Density Function with Approximations 1 and 2 and the Rayleigh Approximation for a Nondimensional Threshold  $r = 1.0$

$r = 1.5$ , 1211 Simulated Events

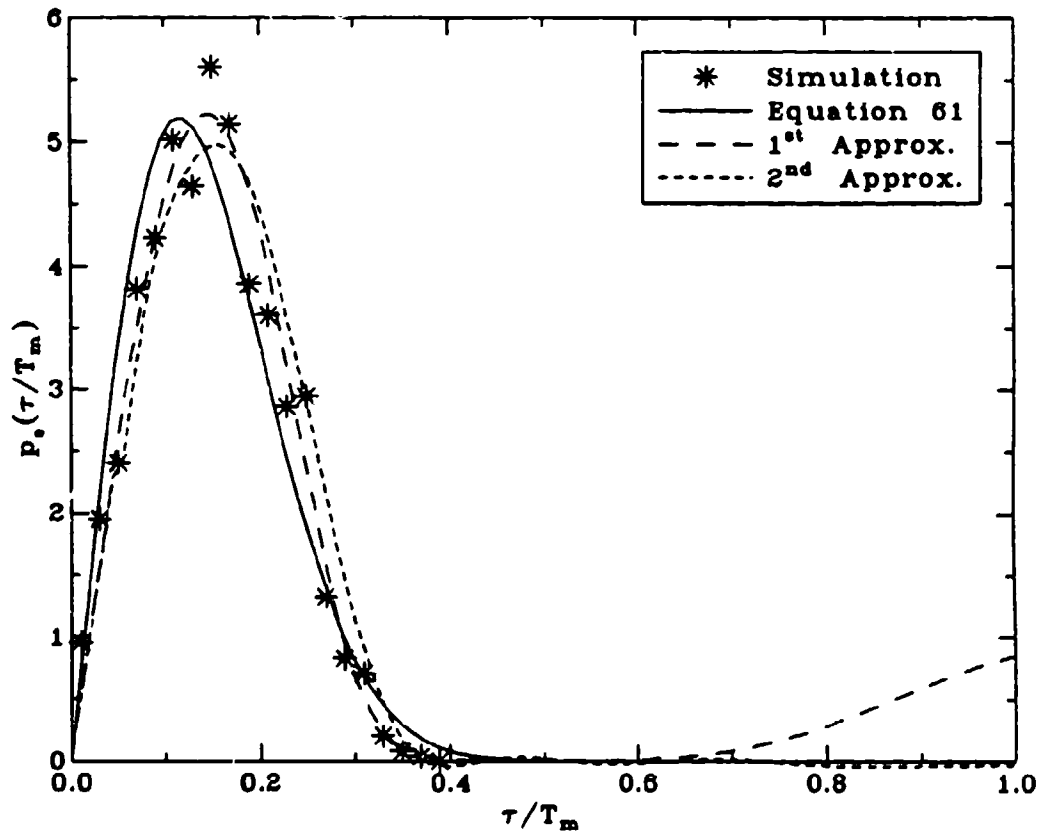


Fig. 16. Comparison of Simulated Threshold Exceedance Probability Density Function with Approximations 1 and 2 and the Rayleigh Approximation for a Nondimensional Threshold  $\tau = 1.5$

$r = 2.0$ , 506 Simulated Events

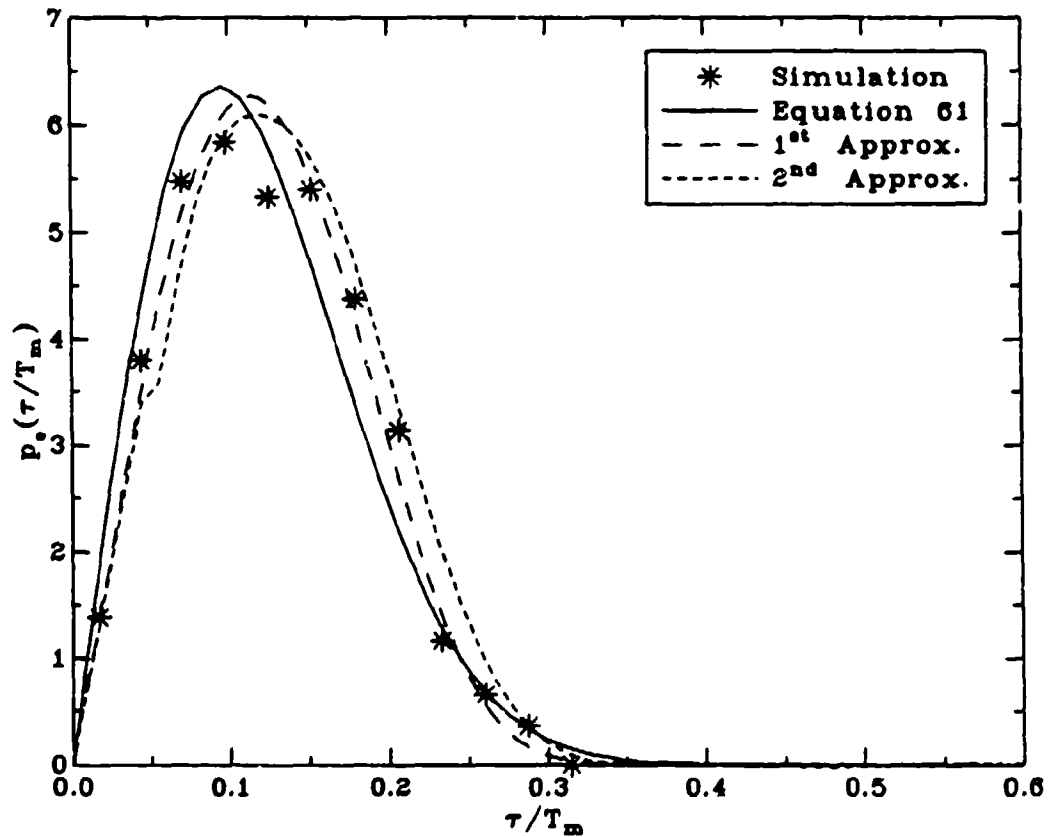


Fig. 17. Comparison of Simulated Threshold Exceedance Probability Density Function with Approximations 1 and 2 and the Rayleigh Approximation for a Nondimensional Threshold  $r = 2.0$

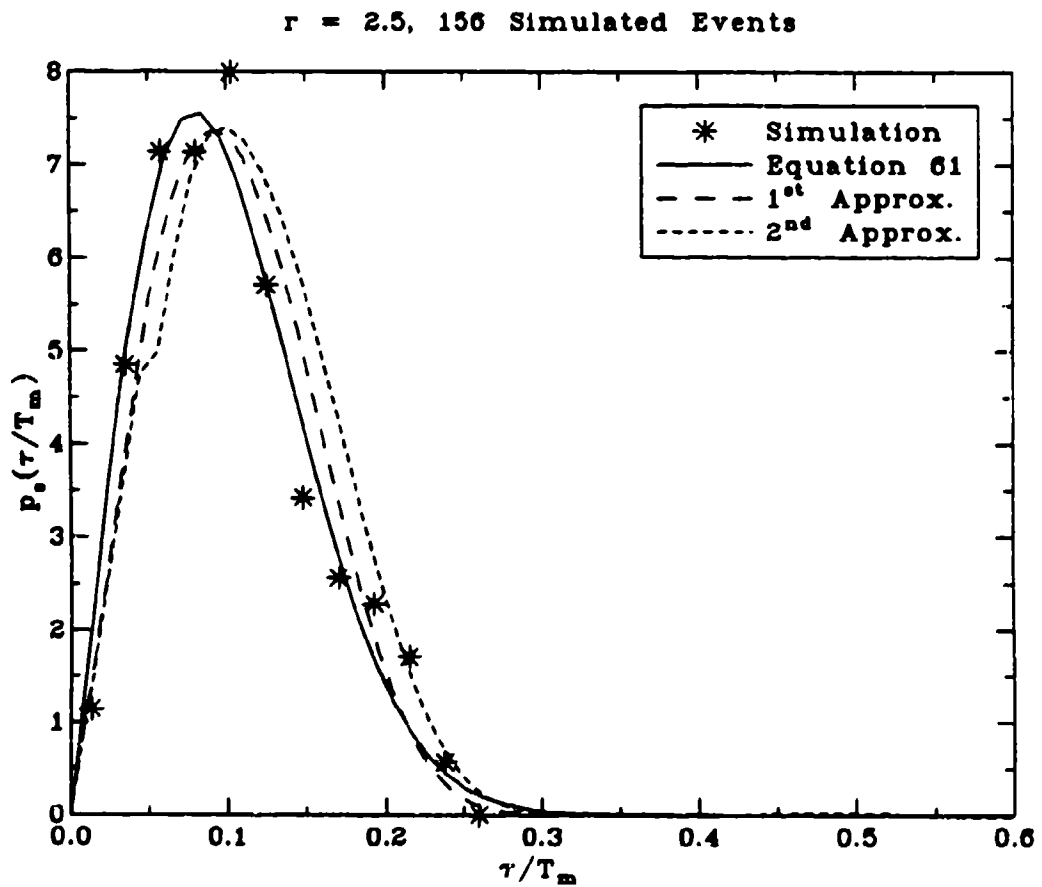


Fig. 18. Comparison of Simulated Threshold Exceedance Probability Density Function with Approximations 1 and 2 and the Rayleigh Approximation for a Nondimensional Threshold  $r = 2.5$

## REFERENCES

1. "U.S. Navy Hindcast Spectral Ocean Wave Model Climatology Atlas: North Atlantic", Naval Oceanography Command Detachment, Asheville, N.C., NAVAIR 50-1C-538 (October 1983).
2. Meyers, W.G., T.R. Applebee, and A.E. Baitis, "User's Manual for the Standard Ship Motion Program SMP", DTNSRDC Technical Report SPD-0936-01 (September 1981).
3. Meyers, W.G. and A.E. Baitis, "SMPS4: Improvements to the Accuracy of the Standard Ship Motion Program SMP81", DTNSRDC Technical Report SPD-0936-04 (September 1985).
4. Smith, T.C. and W.L. Thomas III, "A Survey and Comparison of Criteria for Naval Missions", DTRC Report SHD-1312-01 (October 1989).
5. Baitis, A.E., T.R. Applebee, and T.M. McNamara, "Human Factor Considerations Applied to Operations of the FFG-8 and LAMPS MK III", *Naval Engineers Journal*, Vol. 97, No. 4 (1984).
6. Graham, R., "Motion-Induced Interruptions as Ship Operability Criteria", *Naval Engineers Journal*, Vol. 102, No. 2 (1990).
7. Wei, F.S., Baitis, A.E., and Meyers, W.G.: "Analytical Modeling of SH-2F Helicopter Shipboard Operation", AGARD, Spain (May 1991).
8. Rice, S.O., "Mathematical Analysis of Random Noise", *Bell System Technical Journal*, Vol. 23, 1944, Vol. 24 (1945).
9. Price, W.G. and R.E.D. Bishop, *Probabilistic Theory of Ship Dynamics*, John Wiley & Sons, New York (1974).
10. Shak, M.: "Friction Coefficients of Standardized Panels for Flight Deck Applications", Project No. IT 993, Report No. 12/91, DNASE 4, Canadian Department of National Defence (February 1991).
11. Rice, S.O., "Distribution of the Duration of Fades in Radio Transmission: Gaussian Noise Model", *Bell System Technical Journal*, Vol. 37, No. 3, (1958).
12. Kuznetsov, P.I., Stratonovich, R.L., and Tikhonov, V.I., "On the Durations of Excursions of Random Functions", in: *Non-Linear Transformations of Stochastic Processes*, Edited by P.I. Kuznetsov et al., Pergamon Press, Oxford, (1965).

13. Tikhonov, V.I., "The Distribution of the Duration of Excursions of Normal Fluctuations", in: *Non-Linear Transformations of Stochastic Processes*, Edited by P.I. Kuznetsov et al., Pergamon Press, Oxford, (1965).
14. Ochi, M.K. and Bolton, W.E., "Statistics for Prediction of Ship Performance in a Seaway", *International Shipbuilding Progress*, Vols. 20 and 21, (1973), (1974).
15. Rainal, A.J., "First and Second Passage Times of Rayleigh Processes", *IEEE Transactions on Information Theory*, Vol. IT-33, No. 3, May (1987).
16. Mimaki, T., Tanabe, M. and Wolf, D., "The Multipeak Property of the Distribution Densities of the Level-Crossing Intervals of a Gaussian Random Process", *IEEE Transactions on Information Theory*, Vol. IT-27, No. 4, July (1981).
17. Mimaki, T. and Munakata, T., "Experimental Results on the Level-Crossing Intervals of Gaussian Processes", *IEEE Transactions on Information Theory*, Vol. IT-24, No. 4, July (1978).
18. Vanmarcke, E.H., "On the Distribution of the First-Passage Time for Normal Stationary Random Processes", *Journal of Applied Mechanics*, Vol. 42, Series E, No. 1, March (1975).

**END  
FILMED**

**DATE:** *12-91*

**DTIC**